IN VIVO ANALYSIS OF WILD-TYPE AND VARIANT HUMAN FERROCHELATASES

by

TERESA ADRIANNA COLEMAN ROSS

(Under the Direction of Harry A. Dailey)

ABSTRACT

Ferrochelatase is the terminal enzyme in the heme biosynthetic pathway and catalyzes the insertion of ferrous iron into protoporphyrin IX in the formation of protoheme IX. Little is known about how substrate iron is acquired and taken up by the enzyme or how the enzyme functions at the cellular level. Here we investigated the putative roles of several amino acid residues *in vivo* by constructing and analyzing site-directed mutants within the C-terminus, on the protein surface, and inside the active site of human ferrochelatase. *In vivo* function of the enzyme was assessed by monitoring complementation, cellular growth rates and heme production in a ferrochelatase-deficient strain of *Saccharomyces cerevisiae*. The data suggest a possible surface site that may be involved in ferrochelatase function. These initial *in vivo* characterizations may lead to future advances in identifying specific amino acid residues that play a role in ferrochelatase function.

INDEX WORDS: Ferrochelatase, *in vivo*, *Saccharomyces cerevisiae*,

IN VIVO ANALYSIS OF WILD-TYPE AND VARIANT HUMAN FERROCHELATASES

by

TERESA ADRIANNA COLEMAN ROSS

B.S., Biology, Mars Hill College, 1999

A Thesis Submitted to the Graduate Faculty of The University of Georgia in Partial Fulfillment of the Requirements for the Degree

MASTER OF SCIENCE

ATHENS, GEORGIA

2007

IN VIVO ANALYSIS OF WILD-TYPE AND VARIANT HUMAN FERROCHELATASES

by

TERESA ADRIANNA COLEMAN ROSS

Major Professor: Harry A. Dailey

Committee: Claiborne Glover III
Alan Przybyla

Electronic Version Approved:

Maureen Grasso
Dean of the Graduate School
The University of Georgia
December 2007

DEDICATION

This work is dedicated to the loving memory of my father and brother, Kenneth and Kirk Coleman, to my husband Trevor Ross, and to my mother Lottie Coleman.

ACKNOWLEDGEMENTS

I wish to thank my major professor, Dr. Harry A. Dailey, for allowing me to join his lab and for providing support for me and for this work.

I thank Drs. Claiborne Glover III and Alan Przybyla for not only serving on my committee, but also for believing in me and in my capabilities. Also, I thank Dr. Amy E. Medlock for all of her technical expertise, critical discussions, and extreme willingness to help me.

Lastly, but certainly not least, I would like to express my deepest gratitude to my family and to Rev. Dr. Winfred M. Hope for all of the moral support, constant words of encouragement, and for never letting me give up. Thank you Trevor, mom, Michele, Steven, Audrey, mamma and daddy Ross, and pastor Hope. I love you!

TABLE OF CONTENTS

CHAPTER 1

LITERATURE REVIEW

HEME

Heme production is indispensable for life as it is a major component of a number of hemoproteins that are required for biological processes (Voet and Voet, 2004). Examples include hemoglobin, which binds and carries oxygen from the lungs to the tissues; myoglobin, which binds and carries oxygen in muscles; cytochromes, which transfer electrons in the electron transport chain in cellular respiration (b, c, c_1, a, a_3) as well as detoxify reactive oxygen species (oxidases, peroxidases, catalases) (Grimm, 2003; Ponka, 1997); and nitric oxide synthase, which binds the heme of the receptor guanylyl cyclase in the synthesis of the second messenger nitric oxide (Garrett and Grisham, 1999). Additionally, heme serves as an activator/regulator of transcription factors (Mense and Zhang, 2006) and more recently has been shown to be involved in microRNA processing (Faller et al., 2007). Hence, all living organisms, with the exception of a few obligate pathogens, some anaerobic prokaryotes, and certain auxotrophic unicellular organisms, require the production of heme.

ENZYMES OF HEME SYNTHESIS

Heme is produced in all animal cell types. However, most is produced in erythroid precursor cells for incorporation into hemoglobin and in the liver for

incorporation into other hemoproteins. Mammalian heme synthesis is similar in all cells, with a few tissue-specific differences, and is accomplished through a multi-step process involving eight enzymes that function in the cytoplasm and the mitochondrion (Dailey, 1997; Ferreira, 1995; Ponka, 1997) (Figure 1-1).

The first enzyme, 5-aminolevulinic acid (ALA) synthase (EC 2.3.1.37), functions in the mitochondria and is responsible for catalyzing the condensation of glycine and succinyl-CoA in the formation of ALA. ALA is then transported out of the mitochondria into the cytosol where the next 4 steps are carried out. In the second step of heme biosynthesis, two molecules of ALA are condensed to the asymmetric monopyrrole porphobilinogen (PBG) by the enzyme ALA dehydratase (ALAD) (EC 4.2.1.24), also referred to as PBG synthase (Jordan, 1991a). Through amino acid sequence comparison, it was inferred that the structure of ALAD is highly conserved (Jaffe, 1995). It wasn't until 1997 that the x-ray structure of ALAD was solved at 2.3Å (Erskine et al., 1997). The structure revealed that it consists of 8 monomers folded into an octamer. Each subunit forms a TIM barrel with an extended N-terminal arm (Erskine et al., 2001; Erskine et al., 1997). The arm of each subunit wraps around the adjacent subunit to form dimers. Each dimer consists of one active site which can recognize and bind two substrate ALA molecules (Jaffe, 1995). Four dimers form an octamer which contains a central solvent tunnel. The enzyme has at least two metal-binding sites; one is essential to catalysis while the other plays a structural role (Erskine et al., 2001; Jaffe, 1995). Interestingly, in plants and some bacterial enzymes, the zinc-ligating cysteine residues are absent and are replaced by magnesium-coordinating aspartic acid residues. It is the magnesium ions that are essential to catalysis (Erskine et al., 2001; Jaffe, 1995; Jordan,

1991a). ALAD is sensitive to inactivation by heavy metals such as lead and mercury (Jaffe et al., 1991; Shoolingin-Jordan, 2003). In fact, inhibition of ALAD in red blood cells has been used in the diagnosis of lead poisoning in humans (Chisolm, 1971). Lead poisoning leads to a deficiency in ALAD activity which can subsequently lead to the disease Doss porphyria (Kappas et al., 1995). This disease will be discussed briefly later.

PBG deaminase (EC 4.3.1.8) is the third enzyme involved in the biosynthesis of heme. It is also referred to as hydroxymethylbilane synthase or uroporphyrinogen I synthase and is well characterized. It catalyzes the condensation of 4 PBG molecules by removing 4 amines and forms the linear tetrapyrrole, hydroxymethylbilane (or preuroporphyrinogen) (Jordan, 1990). Nonenzymatic cyclization results in the production of uroporphyrinogen I, which does not serve as a precursor to heme (Kappas et al., 1995). PBG deaminase was the first heme biosynthetic enzyme to have its structure solved (Louie et al., 1992). The *Escherichia coli* structure reveals that there are three domains linked together by flexible strands (Louie et al., 1992). Domains I and II have similar protein folds, whereas domain III has a different fold (Figure 1-3). Domain III is joined to domain I by a long polar helix region. This domain also covalently binds the dipyrromethane cofactor sandwiching it in the catalytic cleft between domains I and II. This cofactor provides an attachment point for the substrate molecules in the formation of the hydroxymethylbilane, analogous to a primer that is elongated in a stepwise mechanism (Hart et al., 1988; Jordan and Warren, 1987; Warren and Jordan, 1988). Preuroporphyrinogen release is likely to occur by reorganization of the active site that allows for cleavage of the enzyme-substrate bonding network. Water then serves as the nucleophile in the hydrolysis and release of the product. The dipyrromethane remains

permanently bound to the enzyme. Since there is only one catalytic site for the condensation of four PBG molecules, the enzyme has been suggested to change conformation to allow for the elongation of the chain to occur (Louie et al., 1996). Enzyme catalysis can be ceased through chain termination. This is known to occur with the inhibitor α-bromoporphobilinogen, whereby the free α-position of PBG has been substituted by bromine, and the enzyme accepts it as a substrate and adds it to any of the intermediates (Warren and Jordan, 1988). A catalytic deficiency may result in the disease acute intermittent porphyria (AIP), which will be discussed briefly later.

Uroporphyrinogen III synthase (UROS), also known as uroporphyrinogen III cosynthetase (EC 4.2.1.75) is the enzyme responsible for rapidly converting the linear tetrapyrrole to the physiologically useful cyclic uroporphyrinogen III. This represents the branch point that separates the heme biosynthetic pathway from corrin biosynthesis (Ajioka et al., 2006; Jordan, 1991a; Kappas et al., 1995). This was the last enzyme in this pathway to be discovered and is the least well characterized. The reaction involves the exclusion of water and the joining of the A and D rings through a spiro-mechanism (Jordan, 1991b; Mathewson and Corwin, 1961). During this process, the orientation of the D ring is flipped. In 2001, the x-ray crystal structure of human UROS was solved at 1.85Å resolution (Mathews et al., 2001). This structure revealed that the enzyme is shaped like a dumbbell whereby it is folded into two α/β domains connected by an anti-parallel β-sheet (Figure 1-4). The N-terminal end (domain I) has a fold similar to a flavodoxin, and domain II resembles a DNA glycosylase-like fold. The active site is located between the two domains within a cleft. Through examination of the crystal structure and mutational analysis, it was concluded that for UROS catalysis there is no

requirement for an acid/base. Instead, catalysis may be affected by acetic- or propionic acid side chains of the substrate or by the involvement of water that is bound to one of the reactive hydroxyl groups of serine, threonine, or tyrosine residues present in the active site (Mathews et al., 2001).

The fifth enzyme in the pathway is uroporphyrinogen decarboxylase (UROD) (EC 4.1.1.37). UROD is responsible for catalyzing the decarboxylation of the 4 acetic acid side chains to methyl groups to form coproporphyrinogen III (Jordan, 1990). This conversion is thought to result from a sequential reaction at low substrate concentrations whereby greater substrate selectivity is favored (Jackson et al., 1976; Jinli and Lim, 1993). The stepwise decarboxylation occurs with the carboxylate group of the four acetic acid side chains being removed prior to the decarboxylation of the A, B, and C rings (Jackson et al., 1976; Jinli and Lim, 1993). High substrate levels seem to lessen enzyme selectivity for each pyrrole ring of UROD, resulting in random decarboxylation (Lash, 1991). All URODs examined have a monomeric molecular weight of 40 kDa, and exist as homodimers (Phillips et al., 1997; Romeo et al., 1986). In eukaryotes, the enzyme is found in the cytoplasm. There is no known requirement for either a coenzyme, metal ions, or prosthetic groups (de Verneuil et al., 1983; Kappas et al., 1995; Straka and Kushner, 1983). The human structure was solved in 1998 at 1.6Å resolution and revealed that it is comprised of a single domain folded into a barrel with a deep cleft that forms the active site (Figure 1-5). There are two active sites per dimer, which face each other. UROD is very specific for an acetic acid side chain and requires an adjacent propionic acid side chain at the β-position. There is a high degree of structural similarity between species of UROD. From modeling experimentation, aspartic acid and tyrosine residues in

the active site were implicated in the decarboxylation mechanism (Martins et al., 2001). The product coproporphyrinogen is transported to the mitochondria where the final 3 steps of heme synthesis take place (Jordan, 1990). A deficiency in UROD activity is associated with the most prevalent human porphyria, porphyria cutanae tarda (Elder and Worwood, 1998)

The antepenultimate enzyme, coproporphyrinogen oxidase (CPO) (EC 1.3.3.3), requires molecular oxygen to catalyze the removal of two carboxylate groups from coproporphyrinogen III, converting the two propionate side chains of rings A and B into vinyl groups forming protoporphyrinogen IX (Akhtar, 2003; Dailey, 2002). There are two forms of this enzyme in living cells, aerobic and anaerobic. Aerobic CPO is found in animals and micro-organisms that are grown aerobically. It has been postulated that this O_2-dependent enzyme catalyzes a metal- and cofactor-independent oxidative decarboxylation whereby it is the molecular oxygen that acts as the electron acceptor (Lee et al., 2005). On the contrary, anaerobic CPO is present in facultative anaerobes and does not require molecular oxygen, but instead uses NAD^+ or $NADP^+$ as an electron acceptor (Dailey, 1990). Additionally, the anaerobic enzyme was identified to be a member of the radical SAM superfamily, which generate catalytic radical species by reductive cleavage of S-adenosylmethionine (SAM) through a [4Fe-4S] cluster (Sofia et al., 2001). The crystal structure of the *E. coli* enzyme was solved in 2003 and reveals the cofactor geometry required for radical SAM catalysis (Layer et al., 2003). Only the O_2-dependent enzyme will be discussed further.

For the oxygen-dependent enzyme, two O_2 molecules are used and two molecules of CO_2 and H_2O_2 are released (Yoshinaga and Sano, 1980). CPO exists primarily as a

homodimer with a molecular weight of ~70 kDa (Grandchamp et al., 1978). In yeast, the enzyme is found in the cytosol, whereas in mammals it contains a mitochondrial targeting sequence that localizes it to the mitochondrial intermembrane space (Dailey et al., 2005). The localization signal is removed during import.

There have been contradictory views on whether or not there is a requirement for a metal cofactor (manganese and copper have been implicated) (Breckau et al., 2003; Camadro et al., 1986; Martasek et al., 1997; Medlock and Dailey, 2004). It is now accepted that CPO carries out its reaction without the need for metals (Martasek et al., 1997; Medlock and Dailey, 2004; Yoshinaga and Sano, 1980), reducing agents, thiols, prosthetic groups, organic cofactors, or modified amino acids (Yoshinaga and Sano, 1980), which makes this a very interesting enzyme. Nonetheless, the first carboxylation has been shown to be the reaction's overall rate-limiting step (Elder and Evans, 1978; Elder et al., 1978). The exact mechanism by which CPO carries out catalysis is still not fully understood.

The crystal structures of both human and yeast O_2-dependant CPO were recently solved by two independent groups (Lee et al., 2005; Phillips et al., 2004). In the yeast structure, the enzyme forms a somewhat flat 7-stranded antiparallel β-sheet that is flanked by α-helices (Figure 1-6). The dimer folds in a way such that the β-sheets face each other. There are two independent active sites per dimer within a deep cleft lined with conserved residues. This cleft is sandwiched between one face of the β-sheet and helices H7-H9. The human enzyme, solved at 1.5A, is nearly identical to the yeast structure.

Protoporphyrinogen oxidase (EC 1.3.3.4) is the penultimate step in the pathway and converts protoporphyrinogen IX into protoporphyrin IX, by oxidizing the tetrapyrrole through the removal of 6 hydrogen atoms. It is the last common enzyme in heme and chlorophyll biosynthesis. It was long debated whether there was a need for an enzymatic reaction to oxidize protoporphyrinogen IX to protoporphyrin IX since autooxidation could occur in the air; however, biochemical and genetic evidence indicates that this reaction is indeed catalyzed in living cells (Falk, 1964; Poulson and Polglase, 1975). Like CPO, there are two forms of this enzyme in nature: aerobic and anaerobic. In aerobic organisms, the oxidation requires 3 molecules of molecular oxygen as the final electron acceptor, which are reduced to H_2O_2 (Akhtar, 2003; Dailey, 1997). The reaction undergoes three two-electron oxidations (Akhtar, 1991). In addition, a non-covalently bound FAD co-factor is required for catalysis (Dailey and Dailey, 1996a; Dailey and Dailey, 1996b). One of the interesting things about this enzyme is that a large class of herbicides are highly specific and efficient at targeting it (Dailey et al., 1994c; Lermontova et al., 1997; Matringe et al., 1989). Since it has been shown that *Bacillus subtilis* PPO is resistant to herbicides, the agrichemical companies have been trying to find ways to design herbicide-resistant forms of the enzyme so that this modified protein may be genetically introduced into crop plants.

The yeast and animal isoforms of PPO are localized to the mitochondria; however, they are not proteolytically cleaved during import (Dailey et al., 1995). In fact, the yeast PPO has been suggested to contain a non-cleavable N-terminal mitochondrial targeting sequence (Camadro and Labbe, 1996). In bacteria the enzyme is bound to the cytoplasmic membrane (Dailey and Dailey, 1996b).

The crystal structure of PPO from tobacco and the prokaryote *Myxococcus xanthus* have been solved by two independent groups (Koch et al., 2004; Corradi et al., 2006). The tobacco structure revealed that it was a homodimer in which each monomer has a molecular mass of 55kDa and contains one non-covalently bound FAD co-factor per monomer (Koch et al., 2004). In plants, however, there are two isoforms of PPO. PPO1 is located in the thylakoid and in the envelope membranes of chloroplasts, and PPO2 is found in the mitochondria bound to the outer surface of the mitochondrial membrane (Ferreira et al., 1988). Only PPO2 will be discussed. There are three structural domains as determined by the crystal structure: i) an FAD-binding domain which displays sequence and structural similarities to other flavoenzymes (Ghisla and Massey, 1989) ii) a planar substrate–binding domain that encloses a narrow active site cavity beneath the FAD and iii) a membrane-binding domain (Figure 1-7) (Koch et al., 2004). The opening of each active site is located on the outside of the dimer near the membrane. It is still unclear whether or not the dimer is formed before or after insertion into the membrane. The membrane-binding domain consists of a U-shaped channel opened at one side leading from the active site into the membrane bilayer. It has been suggested that conserved apolar and charged residues within eight helices anchor the protein to the membrane. The active site is located between the FAD- and substrate-binding domains. Since PPO is located on the intermembrane space side of the inner mitochondrial membrane, and ferrochelatase, the next and final step of the pathway, is associated to the matrix side of the inner mitochondrial membrane, both the substrate and product need to be transported across the inner mitochondrial membrane (Deybach et al., 1985; Ferreira et al., 1988). This cellular organization has resulted in the proposition that

there is a protein-protein interaction between the two proteins which allow for the transport of molecules in and out of the mitochondrial matrix (Ferreira et al., 1988; Proulx and Dailey, 1992). Through model building, Koch et al. (2004) docked the membrane-binding domains onto the ferrochelatase dimer which is located on the opposite side of the membrane. This model implies that there is a tunnel formed between PPO and the active site opening of ferrochelatase which would allow for the transfer of protoporphyrin IX product to ferrochelatase for the insertion of iron in the formation of heme (Figure 1-8). The *M. xanthus* structure has a similar fold to the tobacco structure; however, it primarily differs in its active site composition, namely charge distribution, that results in a different membrane-binding motif. The PPO from *M. xanthus* is similar to that of the eukaryotic enzyme not only because it has similar catalytic properties (to human) but also because it is membrane-bound, dimeric, and is inhibited by the herbicide acifluorfen (Corradi et al., 2006; Dailey and Dailey, 1996a). A deficiency in PPO activity results in the dominantly inheritable disease, commonly referred to as South African disease, variegate porphyria.

The final step in heme synthesis is carried out by ferrochelatase (EC 4.99.1.1). This enzyme is responsible for catalyzing the insertion of ferrous iron into protoporphyrin IX to form heme (Figure 1-9). The current research concentrates on ferrochelatase so more detailed background on this enzyme follows (see below).

Differences and Similarities of Animal and Plant Heme Biosynthesis

Plants utilize the C5 pathway in the biosynthesis of heme. Whereas ALA is directly formed from succinyl Co-A and glycine in animals (and prokaryotes), plants

form ALA enzymatically via a three-step process (Beale and Castelfranco, 1974; Kannangara and Gough, 1979). First glutamate is ligated to $tRNA^{(glu)}$ to form glutamyl-$tRNA^{glu}$ by glutamyl-tRNA synthetase. Subsequently, a NADPH-dependent glutamyl-tRNA reductase catalyzes the production of glutamate 1-semialdehyde (GSA), which is then transaminated to form ALA by GSA-Aminotransferase (Grimm, 2003) (Figure 1-10). The conversion of ALA to protoheme occurs in exactly the same manner as non-plant heme biosynthesis. Additionally, as with animal ferrochelatase, heme exerts a feedback control on plant ALA synthesis (Gough and Kannangara, 1977; Wang et al., 1984; Weinstein and Beale, 1985). For an extensive discussion on heme biosynthesis in plants see (Beale, 1999; Cornah et al., 2003; Moulin and Smith, 2005).

METABOLIC DISEASE

Defects in the enzymes of heme synthesis result in a disease state known as porphyria. The one exception is ALAS, which when deficient is associated with sideroblastic anemia. The porphyrias are classified as either acute or non-acute and result from an overproduction of porphyrin precursors that can occur in any cell type (Scriver, 1989; Stanbury, 1983).

Acute porphyria is accompanied by episodic neurological manifestations, including neuropathic abdominal pain, peripheral neuropathy, and mental disturbances (Anderson et al., 2001). These usually develop during the adult years and are less common in men than in women. Some things that may trigger these symptoms include drugs such as barbituates, endogenous steroid hormones such as progesterone, fasting, dieting, smoking, and stress from illness. All of these factors can increase the demand for

heme production in the hepatocytes and induce the production of the rate-limiting enzyme ALA synthase. The mechanism by which neurologic damage occurs is not fully understood. However, symptoms of the acute porphyrias result primarily from the porphyrin precursors rather than a deficiency of heme (Solis et al., 2004; Soonawalla et al., 2004).

Non-acute porphyrias are characterized by photosensitivity and cutaneous manifestations that result from porphyrins being deposited in the upper epidermal skin layer (Mascaro, 1986; Poh-Fitzpatrick, 1985). Skin lesions may result since porphyrins produce free radicals when exposed to UV light (Sassa, 2006). These symptoms frequently develop in childhood. As with acute porphyrias, non-acute porphyrias are inherited. The only exception is porphyria cutanea tarda (PCT), which is caused by the deficiency of UROD. This disease can be acquired and one of the most potent triggers of its clinical manifestation is alcohol (Moore, 1993). A brief description of the enzyme defects and their associated porphyrias are presented in Table 1-1. For extensive reading on the porphyrias see (Anderson et al., 2001; Dombeck and Satonik, 2005; Kappas et al., 1995; Kauppinen, 2005; Mascaro, 1986; Moore M, 1990; Moore, 1993; Poh-Fitzpatrick, 1985; Sassa, 2006; Stanbury, 1983; Welsh et al., 1995).

FERROCHELATASE

History

The existence of an enzyme responsible for inserting iron into protoporphyrin IX was first described five decades ago in avian erythrocytes (Goldberg et al., 1956). Since then, an abundant amount of information has been gained about the protein and how it

functions, including ferrochelatase from eukaryotic as well as prokaryotic organisms. In the years to follow, Tokunaga et al. (1972) and Kassner et al. (1973) suggested that iron insertion could occur nonenzymatically under physiological conditions; however, this idea was debated two years later. Using a ferrochelatase-deficient strain of bacteria, Dailey and Lascelles (1974) confirmed that this reaction was indeed enzymatic in nature and that there was a true enzyme for the production of heme. Additionally, a ferrochelatase-deficient strain of the budding yeast *Saccharomyces cerevisiae* was also found to require exogenously supplied heme (Gollub et al., 1977).

Purification and Cloning

In the initial stages of studying the enzyme, purification proved a difficult task. This was not only because the protein is expressed at low levels and is membrane bound, but also because of its instability. It was not until the ferrochelatase gene was cloned from *S. cerevisiae* that researchers were able to recombinantly produce and purify sufficient amounts of the enzyme for further study (Labbe-Bois, 1990). Since then, ferrochelatase has been cloned from numerous species ranging from prokaryotic to eukaryotic organisms, including *Escherichia coli (Frustaci and O'Brian, 1993; Miyamoto et al., 1991; Nakahigashi et al., 1991)*, *Bacillus subtilis* (Hansson and Hederstedt, 1992), *Mycobacterium tuberculosis* and *Caulobacter crescentus* (Dailey and Dailey, 2002), the hyperthermophile *Aquifex aelicus* (Wang et al., 2001), *Myxococcus xanthus, Bdellovibrio bacteriovorus, Azotobacter vinelandii,* and *Pseudomonas- syringae, putida, and Porphyromones gingivalis* (Shepherd et al., 2006). Some eukaryotic ferrochelatases that have been cloned include bovine (Shibuya et al., 1995), human (Dailey et al., 1994b;

Nakahashi et al., 1990), mouse (Brenner and Frasier, 1991; Taketani et al., 1990), *S. cerevisiae* (Camadro and Labbe, 1988), *Schizosaccharomyces pombe* (Medlock and Dailey, 2000), as well as chicken and the amphibian *Xenopus laevis* (Day et al., 1998).

The gene for human ferrochelatase has been mapped to chromosome 18.q21.3 (Brenner et al., 1992; Whitcombe et al., 1991).

Primary Structure and Cell Location

Upon examination of the primary sequence of ferrochelatase from various sources, <10% is conserved (Figure 1-11). The conserved residues are suggested to participate in a variety of aspects of the mechanism including proton abstractors (histidine, glutamate, aspartate), metal substrate coordinators (glutamine, arginine, tyrosine) and substrate porphyrin coordinators (arginine, serine, tyrosine) (Dailey and Dailey, 2003a; Dailey et al., 2000; Gora et al., 1996b; Wu et al., 2001).

Three distinct domains are identifiable: First, an amino-terminal extension found in membrane-bound eukaryotic ferrochelatase. This region serves as an organellar targeting sequence, for example the mitochondria in mammals (Karr and Dailey, 1988) and yeast (Camadro and Labbe, 1988; Prasad and Dailey, 1995). Animal ferrochelatases are mitochondrial proteins that are encoded and synthesized in the cytoplasm before being targeted to the mitochondria, via an amino-terminal targeting sequence. Some species that contain the amino-terminal extension have a ferrochelatase that exists in the membrane-bound form, for example human and yeast as well as most eukaryotes and some prokaryotes. In prokaryotes, however, the membrane-bound enzymes are bound to the cellular membrane since they lack organellar membranes. Those ferrochelatases that

lack part of a "lip" region, for example *B. subtilis*, are commonly found as a soluble protein. Upon translocation to the mitochondria, human ferrochelatase undergoes proteolytic processing to its mature size. Subsequently it becomes associated to the matrix side of the inner mitochondrial membrane (Harbin and Dailey, 1985; Jones and Jones, 1969) via a segment of highly conserved hydrophobic residues that are linearly arranged within a "lip" region of the enzyme (Wu et al., 2001). The second domain is a core region consisting of 330 amino acids and is present among all ferrochelatases. The third domain is the carboxy terminal extension which is comprised of 30-50 amino acids. This region is found primarily in eukaryotic ferrochelatases and in some of these eukaryotes is involved in dimerization of the enzyme and coordination of a [2Fe-2S] cluster (Wu et al., 2001).

In contrast to animal ferrochelatase, plant ferrochelatase has two isoforms. One is present in the plastids and mitochondria while the other is found just in chloroplasts (Chow et al., 1998; Hansson et al., 1998; Little, 1976; Suzuki et al., 2000; Suzuki et al., 2002). The two plant isoforms have ~70% sequence homology with the exception of the N-terminal organelle-targeting sequence and the C-terminal segment (Chow et al., 1998). The mitochondrial isoform is found in non-photosynthetic tissues and does not respond to light, whereas the chloroplast ferrochelatase is light responsive. It has been proposed that the C-terminus of the chloroplast isoform mediates membrane binding (Chow et al., 1998). The way in which the ferrochelatase binds to the membrane is similar to a transmembrane motif found in the light-harvesting complex (LHC) protein family (Funk and Vermaas, 1999). The function of the LHC motif is still not fully understood.

Iron Sulfur Cluster

The presence of one [2Fe-2S] cluster per monomer was determined in 1994 by Dailey et al. (1994a) by analysis of UV-visible- and EPR spectra following overexpression of the recombinant human enzyme. The same year ferrochelatase from mouse was also found to contain an iron sulfur cluster (Ferreira et al., 1994). Human ferrochelatase was found to be an unusual [2Fe-2S] cluster-coordinating protein in that its spacing is cys-X_{206}-cys-X_2-cys-X_4-cys, 3 cysteines of which are at the C-terminus and the other of which is located in the core of the protein (Sellers et al., 1998b; Wu et al., 2001) Other [2Fe-2S] cluster-containing proteins, for example ferredoxins, generally have four closely situated cysteines that serve as ligating residues. Interestingly, the ferrochelatase from *S. cerevisiae*, although it contains the carboxy terminal extension, does not contain C-terminal cysteines nor does it posses an iron sulfur cluster. In contrast, the yeast *S. pombe* contains the carboxy terminal extension, C-terminal cysteins, and posses the cluster (Medlock and Dailey, 2000). In human ferrochelatase, mutagenesis showed that elimination of any one of the ligating cysteines prevents the cluster from forming causing the enzyme to become inactive (Dailey et al., 1994a; Sellers et al., 1998b). Through studies examining the functionality of chimeric mutants consisting of human and yeast sequence regions, it is clear that actual enzyme activity is not strictly dependant on the presence of the cluster (Dailey and Dailey, 2003a; Medlock and Dailey, 2000).

It was initially thought that there were no C-terminal extensions that functioned in coordinating iron sulfur clusters in microbial ferrochelatases. However, as more sequence information became available, a number of organisms were found to contain [2Fe-2S] clusters. Upon expressing, purifying, and characterizing two bacterial

ferrochelatases that contain the C-terminus and four cysteines, Dailey and Dailey (2002) provided the first evidence that iron-sulfur clusters exist in some microbial ferrochelatases. These include *Caulobacter crescentus,* a membrane-associated homodimer, and the soluble *Mycobacterium tuberculosis*. Since then, a new class of [2Fe-2S] cluster-containing ferrochelatases have been identified by site-directed mutagenesis (Dailey and Dailey, 2003a; Shepherd et al., 2006). These results showed that in some species, the cluster is coordinated by four cysteines within an internal amino acid insertion segment of approximately 20 residues, which is quite different from that of human ferrochelatase. These include the ferrochelatases from *Myxococcus xanthus, Bdellovibrio bacteriovorus, Pseudomonas aruginosa,* and by sequence similarity *Azotobacter vinelandii* (Dailey and Dailey, 2003a; Shepherd et al., 2006).

Although the role of the cluster is still largely unknown, the iron from the cluster is not used as substrate iron (Dailey and Dailey, 2003a). A possible role for the cluster in human ferrochelatase as proposed by Sellers et al. (1996) is a sensor for nitric oxide. This has been suggested from studies using purified recombinant human ferrochelatase to analyze the effect that NO has on the iron sulfur cluster. EPR and UV-visible absorption showed that ferrochelatase is inactivated by low concentrations of NO, which is mediated via destruction of the cluster. The authors furthermore concluded that this NO regulation may be a component of the overall regulation of iron metabolism. The [2Fe-2S] clusters in microbial ferrochelatases are more stable and in air, but are destroyed by NO (unpublished results).

Crystal Structure

The first structure of any ferrochelatase to be solved was that of the bacterium *B. subtilis* by Al-Karadaghi et al. (1997). *B. subtilis* ferrochelatase contains no cluster, lacks a C-terminal extension, is a small (36 kDa) water-soluble protein, and functions in the monomeric form (Al-Karadaghi et al., 1997). Three years later, the crystal structure of human ferrochelatase was solved (Wu et al., 2001), followed by *S. cerevisiae* in 2002 (Karlberg et al., 2002). The major difference between the ferrochelatase from *B. subtilis* and that from human is the area around the active site pocket (Al-Karadaghi et al., 1997; Wu et al., 2001). At the entrance to the active site pocket, the human enzyme contains an "upper lip" region consisting of residues 90-130. This lip region there is a hydrophobic 13-residue insertion that is absent in the *B. subtilis* enzyme. Previous studies have suggested both a monomeric and a dimeric human structure; however, Dailey's group, through their crystallization data settled this dispute as they found that it was indeed a homodimer with a molecular weight of approximately 86 kDa (Burden et al., 1999; Dailey et al., 1994a; Wu et al., 2001) (Figure 1-12). Structural determination also confirmed the presence of the [2Fe-2S] cluster along with its coordination motif.

The human structure reveals that the enzyme is folded into α/β domains, including 17 helices and 8 β-sheets. Furthermore, the iron sulfur cluster is coordinated by C196, C403, C406, and C411 and anchors the C-terminus to the rest of the monomer through the coordination by C196 in the N-terminal domain (Figure 1-12). Additionally, the cluster is indirectly involved in dimerization since the C-terminus participates in hydrogen bond networks at the dimer interface (Crouse et al., 1996; Dailey et al., 1994a; Sellers et al., 1998b; Wu et al., 2001).

Active Site Pocket

The protein is found associated with the inner mitochondrial membrane which is proposed to be through two hydrophobic lips (an upper lip, residues 90-130; and lower lip, residues 300-311) that form the entrance to the active site pocket (Figure 1-13) (Dailey and Dailey, 2003a; Wu et al., 2001). As seen in the crystal structure, the active site can be accessed through the membrane-associated surface (or lip opening) (Wu et al., 2001). Lining the interior of the active site are hydrophilic residues that are highly conserved among species (Table 1-2). Furthermore, there is a path of acidic residues leading from the surface to the invariant active site histidine that may be involved in proton abstraction from porphyrin (Sellers et al., 2001; Wu et al., 2001). By site-directed mutagenesis and kinetic analysis, the active site H263 has been shown to be essential for catalysis (Gora et al., 1996b; Sellers et al., 2001; Wu et al., 2001). Also in the active site are an arginine and tyrosine residue that were proposed to be involved in metal binding and specificity (Sellers et al., 2001; Wu et al., 2001). These residues, R164 and Y165, are located on the opposite side of the pocket from H263, and when mutated to leucine and phenyalanine, respectively, show an altered affinity for iron without an alteration in porphyrin affinity (Sellers et al., 2001). Furthermore, mutating both residues simultaneously results in nearly undetectable levels of activity (Sellers et al., 2001). Collectively, these data suggest that these residues play a key role in substrate iron binding and catalysis.

Since the structure determination of human ferrochelatase, a variety of mutant forms have been solved, including the surface mutant H240A (Missaoui et al., unpublished results), upper lip mutant F110A, which co-purifies with heme (Medlock et

al., 2007), and active site mutant E343K with substrate protoporphyrin bound in the active site (Medlock et al., 2007b). E343K will be discussed later.

Substrate Specificity

Ferrochelatase can utilize a number of both porphyrin and metal substrates. The IX isomer porphyrins that are capable of being used include its natural substrate, protoporphyrin, along with hemato-, meso-, and deuteroporphyrin (protoporphyrin being the least soluble, and deuteroporphyrin being the most) (Dailey et al., 1989; Honeybourne et al., 1979). The kinetic constants for the porphyrins vary when making comparisons from lab to lab due to procedural differences. Generally, the apparent K_ms are 1-15 μM, 10-40 μM, and 40-250 μM for protoporphyrin, mesoporphyrin, and deuteroporphyrin, respectively (Dailey, 1997; Dailey and Dailey, 2003a).

Substrate metal is also variable. Although the physiologic metal is iron, mammalian ferrochelatase can utilize divalent cobalt and zinc with apparent K_ms of iron and cobalt being in the range of 10 μM (Dailey, 1997; Dailey and Dailey, 2003a). It should be noted that only the ferrous form of iron can be utilized and not ferric iron, although ferric iron does not inhibit the protein (Dailey, 1990). In contrast, metal specificity differs in some bacterial ferrochelatases. For instance, *B subtilis* can utilize divalent copper and zinc, but not cobalt (Dailey, 1990; Dailey, 1996). How ferrochelatase dictates metal ion selectivity and specificity remains to be determined. It has been proposed that chelatases impose metal specificity by distorting the substrate porphyrin ring differently (Al-Karadaghi et al., 2006).

SUBSTRATE BINDING

Porphyrin Binding

It was originally proposed that the two terminal enzymes, PPO and ferrochelatase, of the heme pathway form a transient complex in the production of heme (Ferreira et al., 1988). This was demonstrated by kinetic analysis of the two enzymes in mitochondrial membranes. There was no increase in heme production when low concentrations of substrate porphyrin were supplied. The authors concluded that since the exogenously supplied porphyrin did not compete for endogenous porphyrin and result in more heme production, then substrate/product is channeled between the two enzymes. The idea that channeling was required was abandoned when Proulx et al. (1992) found that in isolated murine mitochondria, radiolabeled substrate protoporphyrin can compete for endogenous protoporphyrin in the formation of heme, although endogenously generated substrates were more effective. Since the model of complex formation is so appealing, more studies have been done in order to provide support for such a model. In 2004, Koch et al., through examining the crystal structure of tobacco propoporphyrinogen oxidase, the preceding enzyme in the pathway, along with model building and docking experiments, suggested that channeling can occur between the terminal enzymes. In their model, the membrane-binding domain of PPO, which is proposed to contain a U-shaped channel with its active site openimg into the membrane bilayer, is where the protoporphyrin IX is translocated into ferrochelatase. In this model, there is an overlap of the channel openings of PPO and ferrochelatase which would allow for porphyrin substrate to easily exit PPO and enter the ferrochelatase active site (Koch et al., 2004) (Fig 1-8). Other studies with human ferrochelatase have likewise unraveled how substrate protoporphyrin

is partitioned into the active site through the membrane-facing side of the protein (Medlock et al., 2007b; Wu et al., 2001). In order to understand the mechanism for the selectivity of ferrochelatase binding to porphyrin, Dailey and Fleming (1986) investigated the role of arginyl residues by chemical modification of purified recombinant bovine ferrochelatase since these residues are frequently found in heme-binding proteins as binding protoheme. Results showed that modification of arginyl residues resulted in loss of activity. Collectively, they provided evidence that one arginine in particular is involved in binding of substrate porphyrin; however, that arginine does not act alone, and there may be other residues involved (Dailey and Fleming, 1986).

Some non-substrate porphyrins, such as alkylated porphyrins, have been shown to competitively inhibit ferrochelatase activity *in vivo* and *in vitro* (Dailey and Fleming, 1983; De Matteis et al., 1980). It is known that the alkylated pyrrole ring tilts out of plane approximately 30º (Goldberg and Thomas, 1976; Lavallee, 1987), thereby leading to the proposal that the bent N-alkylated porphyrins may be representative of a transition state analog for porphyrin iron insertion (Dailey, 1990; Dailey et al., 1989; Lavallee, 1988). This was supported by Takeda et al. (1992) whose kinetic data showed an increased rate of metalation into distorted porphyrins, and Cochran and Schultz (1990), who showed that ferrochelatase-like activity resulted from antibody raised against an N-methylmesoporphyrin. Furthermore, Blackwood et al. (1988) showed through resonance Raman studies that ferrochelatase-induced porphyrin distortion was different from the tilting of a single ring in the N-alkylated porphyrins, suggesting that N-methylmesoporphyrin is indeed inhibitory. To add support, Lecerof et al. (2000) provided a crystal structure of *B. sub*tilis ferrochelatase in complex with the potent

inhibitor N-methylmesoporphyrin in the active site. It is noteworthy to mention that different ferrochelatases are differentially sensitive to N-alkyl porphyrin inhibition (Marks, 1987; Marks et al., 1985).

Recently, the crystal structure of the human ferrochelatase variant E343Kwas solved at 2.5Å (Medlock et al., 2007b). This variant co-purifies with substrate protoporphyrin IX, and the structure disproves the theory of how the porphyrin is bound to the active site based on previous crystallographic studies that showed the orientation of N-methylmesoporphyrin in the active site of *B. subtilis* ferrochelatase (Lecerof et al., 2000). These new data clearly show that N-methylmesoporphyrin does not mimic the coordination of the physiologic porphyrin substrate nor is the N-alkylated porphyrin a transition state analog (Medlock et al., 2007b). To ensure the porphyrin is bound in the active site with a snug fit, one of the propionates forms a salt bridge with R115 and another forms hydrogen bonds with the side chains of residues Y123 and S130 (Medlock et al., 2007b). When comparing porphyrin-bound and unbound forms of human ferrochelatase, the structure reveals that the active site mouth is closed in the bound form. Furthermore, the spatial positions of residues 302-313 and 349-361 (located within loop regions near the entrance to the active site), along with numerous amino acid side chains within the active site (M76, R164, F337, H341), have conformational alterations with substrate bound (Dailey et al., 2007; Medlock et al., 2007b) (Figure 1-14). These alterations cause the porphyrin to become engulfed by the protein within the active site pocket thus closing the pocket around the porphyrin pyrrole. How heme exits the active site of ferrochelatase, once metalation of the pyrrole occurs, is still unclear, however it

has been suggested that heme may be released through an opening created by structural alteration of a conserved π-helix (Medlock et al., 2007a).

Metal Binding

The mechanism of ferrochelatase-metal binding is still not fully understood. In eukaryotes, cellular iron may be endocytosed from the cell surface via transferrin receptors. Iron is transported to the mitochondria where it can be used in a number of metabolic pathways, including heme synthesis, or stored in mitochondrial ferritin (Napier et al., 2005). Surplus iron is bound to ferritin within the cytosol. Recent data identify mitoferrin, a member of the vertebrate mitochondrial solute carrier family, as the protein possibly responsible for importing iron into the mitochondrial matrix for heme biosynthesis (Muhlenhoff et al., 2003; Shaw et al., 2006b; Zhang et al., 2005). The exact mechanism of how the iron is acquired by ferrochelatase for incorporation into the tetrapyrrole center remains to be determined. Since the cation does not diffuse through the phospholipid membrane, and because it is not free in the cellbecause of its potential toxicity, it is possible that mitoferrin, an integral membrane protein, interacts directly with ferrochelatase to deliver the ferrous ion. Iron that is acquired by ferrochelatase and translocated to the active site must be bound to the final active site residue loosely enough to allow for metalation of the porphyrin. From kinetic studies, the Dailey lab has identified some residues as having a proposed role in iron binding. Sellers et al. (2001) proposed a model whereby initial iron binding may occur on the matrix-facing surface of the enzyme at residues H231 and D383. This site was identified in the crystal structure as a site for exogenously supplied cobalt, based on soaking experiments (Sellers et al.,

2001). From there the metal is passed along a series of conserved residues to the active site H263 that is thought to serve as the proton abstractor for porphyrin metalation (Sellers et al., 2001). In another model based on kinetic analysis, it was proposed that the iron may initially bind to the surface H240 residue for subsequent passage through a tunnel of conserved residues that leads to the active site (Missaoui, unpublished results). Both models support the proposition that there exists a donor protein that docks on ferrochelatase at a surface site on the matrix side of the protein and subsequently delivers the iron to its partner (Dailey and Dailey, 2003a). Continued studies to investigate possible regions of ferrochelatase where the iron is acquired or where the putative iron donor, perhaps mitoferrin, might dock would help to support a model for iron acquisition.

CATALYSIS

The catalytic mechanism for all known ferrochelatases is highly conserved. Porphyrin metalation is proposed to occur through a sequential bi-bi reaction whereby iron binds first followed by porphyrin binding and distortion (Dailey and Fleming, 1983; Hoggins et al., 2007): Once the metal is translocated to the active site, it forms a "sitting-atop" complex on the tetrapyrrole and inserts into the distorted porphyrin (Hambright, 1975; Takeda et al., 1992). Metalation then occurs via residues R164 and Y165 (Sellers et al., 2001). The conserved H263 residue is the initial proton acceptor. Two protons are passed to the conserved residues D340, H341, and E343 for the concomitant release with iron-protoporphyrin formation (Dailey, 1990; Dailey, 1996; Lavallee, 1988; Sellers et al., 2001).

In addition to enzyme-catalyzed insertion of metal into porphyrin, it has been shown that metalation can occur non-enzymatically. This includes anti-N-methylmesoporphyrin antibody-catalyzed porphyrin metalation at a rate of 10% of metalation with ferrochelatase (Cochran and Schultz, 1990). This nonenzymatic metalation is made possible because the antibody binds mesoporphyrin causing the porphyrin to distort as shown by resonance Raman studies (Blackwood et al., 1998). Other types of nonenzymatic metalation that have been reported include DNA- and RNAzyme catalyzed reactions (Conn et al., 1996; Li and Sen, 1996).

ERYTHROPOIETIC PROTOPORPHYRIA

Defects in ferrochelatase enzyme results in an autosomal dominant inherited disease know as erythropoietic protoporphyria (EPP). This disease was first described by Magness et al. (1961). Over a decade later, Bonkowsky et al. (1975) provided the first evidence that EPP results from subnormal enzyme activity causing a build-up of protoporphyrin IX substrate. Researchers are now trying to understand the symptoms and the clinical effects of the different mutations in the ferrochelatase gene that lead to enzyme deficiency and consequently the disease. EPP is the third most common porphyria after acute intermittent porphyria and porphyria cutanae tarda, and is the most common erythropoietic porphyria (Sassa, 2006).

Clinical Manifestations

The major symptom of EPP is a painful dermatologic sensitivity to light resulting in skin lesions. Common reported symptoms include burning, tingling, itching, painful erythema and swelling, and mild scarring upon brief exposure to sunlight (Poh-

Fitzpatrick, 1984; Scholnick et al., 1971). This is the result of accumulated protoporphyrin, mainly found in erythropoietic tissues, that is deposited in the skin, including the face and hands (Moore and Wintrobe, 1987). The excess protoporphyrin in tissues is primarily found in the reticulocytes of bone marrow and is excreted in feces (Poh-Fitzpatrick, 1984). In contrast to other porphyrias, the excess porphyrin is not increased nor excreted in urine due to its insolubility (Magnus et al., 1961; Poh-Fitzpatrick, 1984). Although the photosensitivity aspect of the disease is not life threatening, in <5% of patients the protoporphyrin accumulation crystallizes and causes a blockage of biliary passages. Furthermore, in some cases liver dysfunction followed by liver failure will occur and cirrhosis may develop. In this case without a liver transplant, the condition is fatal (Bloomer et al., 1998). Patients with EPP therefore must limit their exposure to sunlight to avoid episodes and accompanied cutaneous lesions. Most symptoms start in early childhood. EPP is the most common of the erythropoietic porphyrias and is more common in Caucasians; however it can occur in patients from other races (Scriver, 1989).

Inheritance and Mutations

In EPP, one would expect a 50% reduction in ferrochelatase activity since it is a dominantly inherited disease. However, most frequently, only 25% of normal activity exists in patients with the disease (Dailey et al., 2000). There have been a number of suggestions as to why this may be the case. These include the presence of a third allele, low expression of the wild-type allele, dysfunctional dimerization with the mutant proteins, and diet or environmental factors (Dailey et al., 2000; Gouya et al., 2006;

Magness et al., 2000). Since the inheritance has much been debated and shown to be more complex than initially thought, it has now been classified and favored as being autosomal dominant associated with incomplete penetrance since <10% of the carriers of a gene mutation will show clinical symptoms of the disease (Schneider-Yin et al., 2001). The most current suggestion for the variation in ferrochelatase activity in EPP patients was given by Gouya et al. (1996, 1999). In this model the variation is due to coinheritance of a mutated ferrochelatase allele accompanied with a weakly expressed normal allele (Gouya et al., 1996; Gouya et al., 1999). Furthermore, the penetrance of the dominant nature of the mutation may be modulated by functional polymorphisms that occur at the same locus (Gouya et al., 2006)

To date, over 88 EPP mutations have been described (Human Genome Mutation Database; Di Pierro et al. 2007). Included are missense/nonsense, and frameshift mutations that result in gene splicing abnormalities that subsequently lead to intragenic deletions and early termination of translation (Di Pierro, 2007; Sellers et al., 1998a; Sellers et al., 1998b). Additionally, amino acid substitutions and early polypeptide chain termination mutations as well as nonsense mutations associated with functional deficiency of ferrochelatase have been described (Brenner et al., 1992; Di Pierro, 2007; Ostasiewicz et al., 1995; Schneider-Yin et al., 2000; Todd, 1998). Some EPP mutations have been shown to cause protein structural instability by preventing iron-sulfur cluster formation and subsequently the inability to dimerize, leading to inactivity of the enzyme (Najahi-Missaoui and Dailey, 2005; Sellers et al., 1998a).

Treatment

A number of treatments for EPP have been useful. These include oral administration of high doses of β-carotene to minimize sun sensitivity, and the use of porphyrin absorbents such as cholestyramine to reduce plasma protoporphyrin levels and to possibly slow the progression of the liver disease (Mathews-Roth et al., 1977; Moore M, 1990). Some therapeutic treatments described include red blood cell transfusions, exchange transfusion, and intravenous administration of haematin to suppress protoporphyrin production, as well as liver transplantation. Although liver transplantation can be beneficial, it may be considered to be a temporary fix since the new liver is still susceptible to protoporphyrin-induced damage (Bloomer et al., 1996; Sassa, 2006).

To unravel the molecular aspect of the uncharacteristic decrease in ferrochelatase activity of EPP, Missaoui and Dailey (2005) provided the first investigation of the activity and physical properties of homo- and heterodimeric ferrochelatase mutants. In this study, they showed that mutations in ferrochelatase that cause EPP can result from protein structural changes that are associated with enzyme activity that may in some instances be affiliated with the loss of the iron sulfur cluster (Najahi-Missaoui and Dailey, 2005). Furthermore, they showed that some of the mutations resulted in more than 50% of wild-type activity levels. They concluded that there is no real correlation between the gene defect and the activity displayed suggesting that there may be other factors that need to be considered. These include associations with other mutations as well as environmental factors.

RESEARCH OBJECTIVES

A plethora of work has been done to elucidate the mechanism of ferrochelatase function by studying a number of species, both prokaryotic and eukaryotic. However, Abbas et al. (1993), Gora et al. (1996), and Olssen et al. (2002), made the first attempts at studying ferrochelatase function *in vivo* using yeast (Abbas and Labbe-Bois, 1993; Gora et al., 1996b) and *B. subtilis (Olsson et al., 2002)* host systems. This is important because although we can gain numerous insights into the protein mechanisms and substrate binding/coordination through *in vitro* methodologies, it is important to corroborate these findings with *in vivo* methodologies. It is reasonable to say that there may be discrepancies in what is seen with *in vitro* analyses and what really happens inside the cell. A simple reason is because the complete system required for iron metabolism, in terms of ferrochelatase, is not required when carrying out activity assays since substrate can possibly enter the active site without the need for a donor protein. By studying mutants of the *B. subtilis* and yeast enzymes, it was shown that there were some discrepancies between *in vitro* and *in vivo* function. Some of the mutants functioned normally *in vitro*; however, *in vivo* they had defects in cell growth, heme production, as well as an accumulation of porphyrin (Gora et al., 1996b; Olsson et al., 2002). Therefore, with *in vivo* analysis, one can get a more complete picture of what really happens under physiological conditions. In the studies by Olsson et al. (2002) and Gora et al. (1996), the function of several residues was postulated based on site-directed mutagenesis and activity measurements in terms of functionality. In the current study, we report the first investigation of human ferrochelatase using *in vivo* methodologies. Here, the function of ferrochelatase surface, as well as active site mutants was investigated to gain knowledge

of the cellular effects on activity. The major goal was to develop a system whereby we utilize a ferrochelatase-deficient (*Δhem15*) strain of yeast to identify and characterize mutants that may be involved in ferrochelatase function.

REFERENCES

Abbas, A., and Labbe-Bois, R. (1993). Structure-function studies of yeast ferrochelatase. Identification and functional analysis of amino acid substitutions that increase Vmax and the KM for both substrates. J Biol Chem *268*, 8541-8546.

Ajioka, R. S., Phillips, J. D., and Kushner, J. P. (2006). Biosynthesis of heme in mammals. Biochim Biophys Acta *1763*, 723-736.

Akhtar, M. (1991). Mechanism and stereochemistry of the enzymes involved in the conversion of uroporphyrinogen III into haem, In Biosynthesis of Tetrapyrroles, P. M. Jordan, ed. (Amsterdam ; New York: Elsevier), pp. xii, 309.

Akhtar, M. (2003). Coproporphyrinogen III and Protoporphyrin IX Oxidases, In The Porphyrin Handbook, K. M. Kadish, Smith, K.M., Guillard, R., ed. (California, USA: Elsevier Science), pp. 75-92.

Al-Karadaghi, S., Franco, R., Hansson, M., Shelnutt, J. A., Isaya, G., and Ferreira, G. C. (2006). Chelatases: distort to select? Trends Biochem Sci *31*, 135-142.

Al-Karadaghi, S., Hansson, M., Nikonov, S., Jonsson, B., and Hederstedt, L. (1997). Crystal structure of ferrochelatase: the terminal enzyme in heme biosynthesis. Structure *5*, 1501-1510.

Anderson, K. E., Sassa, S., Bishop, D. F., and Desnick, R. J. (2001). Disorders of heme biosynthesis: X-linked sideroblastic anemia and the porphyrias, In The Metabolic and Molecular Bases of Inherited Disease, C. Scriver, Beauder, A., Sly, W., Valle, D., Childs, B., Kinzler, K., Vogelstein, B., ed. (New York: McGraw-Hill), pp. 2991-3062.

Beale, S. I. (1999). Enzymes of chlorophyll biosynthesis. Photosynth Res *60*, 43-73.

Beale, S. I., and Castelfranco, P. A. (1974). The biosynthesis of d-aminolevulinic acid in higher plants I. Accumulation of d-aminolevulinic acid in greening plant tissues 1. Plant Physiol *53*, 291-296.

Blackwood, M. E., Jr., Rush, T. S., 3rd, Romesberg, F., Schultz, P. G., and Spiro, T. G. (1998). Alternative modes of substrate distortion in enzyme and antibody catalyzed ferrochelation reactions. Biochemistry *37*, 779-782.

Bloomer, J., Bruzzone, C., Zhu, L., Scarlett, Y., Magness, S., and Brenner, D. (1998). Molecular defects in ferrochelatase in patients with protoporphyria requiring liver transplantation. J Clin Invest *102*, 107-114.

Bloomer, J. R., Rank, J. M., Payne, W. D., and Snover, D. C. (1996). Follow-up after liver transplantation for protoporphyric liver disease. Liver Transpl Surg *2*, 269-274.

Breckau, D., Mahlitz, E., Sauerwald, A., Layer, G., and Jahn, D. (2003). Oxygen-dependent coproporphyrinogen III oxidase (*HemF*) from *Escherichia coli* Is stimulated by manganese. J Biol Chem *278*, 46625-46631.

Brenner, D. A., Didier, J. M., Frasier, F., Christensen, S. R., Evans, G. A., and Dailey, H. A. (1992). A molecular defect in human protoporphyria. Am J Hum Genet *50*, 1203-1210.

Brenner, D. A., and Frasier, F. (1991). Cloning of murine ferrochelatase. Proc Natl Acad Sci USA *88*, 849-853.

Burden, A. E., Wu, C., Dailey, T. A., Busch, J. L., Dhawan, I. K., Rose, J. P., Wang, B., and Dailey, H. A. (1999). Human ferrochelatase: crystallization, characterization of the [2Fe-2S] cluster and determination that the enzyme is a homodimer. Biochim Biophys Acta *1435*, 191-197.

Camadro, J. M., Chambon, H., Jolles, J., and Labbe, P. (1986). Purification and properties of coproporphyrinogen oxidase from the yeast *Saccharomyces cerevisiae*. Eur J Biochem *156*, 579-587.

Camadro, J. M., and Labbe, P. (1988). Purification and properties of ferrochelatase from the yeast Saccharomyces cerevisiae. Evidence for a precursor form of the protein. J Biol Chem *263*, 11675-11682.

Camadro, J. M., and Labbe, P. (1996). Cloning and characterization of the yeast *HEM14* gene coding for protoporphyrinogen oxidase, the molecular target of diphenyl ether-type herbicides. J Biol Chem *271*, 9120.

Chisolm, J., J.J. (1971). Lead poisoning. Sci Am *224*, 15-23.

Chow, K. S., Singh, D. P., Walker, A. R., and Smith, A. G. (1998). Two different genes encode ferrochelatase in arabidopsis: mapping, expression and subcellular targeting of the precursor proteins. Plant J *15*, 531-541.

Cochran, A. G., and Schultz, P. G. (1990). Antibody-catalyzed porphyrin metallation. Science *249*, 781-783.

Conn, M. M., Prudent, J. R., and Schultz, P. G. (1996). Porphyrin metalation catalyzed by a small RNA molecule. J Am Chem Soc *118*, 7012–7013.

Cornah, J. E., Terry, M. J., and Smith, A. G. (2003). Green or red: what stops the traffic in the tetrapyrrole pathway? Trends Plant Sci *8*, 224-230.

Corradi, H. R., Corrigall, A. V., Boix, E., Mohan, C. G., Sturrock, E. D., Meissner, P. N., and Acharya, K. R. (2006). Crystal structure of protoporphyrinogen oxidase from *Myxococcus xanthus* and its complex with the inhibitor acifluorfen. J Biol Chem *281*, 38625-38633.

Crouse, B. R., Sellers, V. M., Finnegan, M. G., Dailey, H. A., and Johnson, M. K. (1996). Site-directed mutagenesis and spectroscopic characterization of human ferrochelatase: identification of residues coordinating the [2Fe-2S] cluster. Biochemistry *35*, 16222-16229.

Dailey, H. A. (1990). Conversion of coproporphyrinogen to protoheme in higher eukaryoes and bacteria, In Biosynthesis of heme and chlorophylls H. A. Dailey, ed. (New York: McGraw-Hill), pp. 123-163.

Dailey, H. A. (1996). Ferrochelatase, In Mechanisms of metallocenter assembly, E. G. L. Hausinger R.P., Marzilli, L.G. , ed. (New York: VCH), pp. 77-98.

Dailey, H. A. (1997). Enzymes of heme biosynthesis. J Biol Inorg Chem *V2*, 411-417.

Dailey, H. A. (2002). Terminal steps of haem biosynthesis. Biochem Soc Trans *30*, 590-595.

Dailey, H. A., and Dailey, T. (2003). Ferrochelatase, In The Porphyrin Handbook, K. M. Kadish, Smith, K.M., Guillard, R., ed. (California, USA: Elsevier Science), pp. 93-121.

Dailey, H. A., and Dailey, T. A. (1996a). Protoporphyrinogen oxidase of *Myxococcus xanthus*. J Biol Chem *271*, 8714-8718.

Dailey, H. A., Dailey, T. A., Wu, C. K., Medlock, A. E., Wang, K. F., Rose, J. P., and Wang, B. C. (2000). Ferrochelatase at the millennium: structures, mechanisms and [2Fe-2S] clusters. Cell Mol Life Sci: CMLS *57*, 1909-1926.

Dailey, H. A., Finnegan, M. G., and Johnson, M. K. (1994a). Human ferrochelatase is an iron-sulfur protein. Biochemistry *33*, 403-407.

Dailey, H. A., and Fleming, J. E. (1983). Bovine ferrochelatase. Kinetic analysis of inhibition by N-methylprotoporphyrin, manganese, and heme. J Biol Chem *258*, 11453-11459.

Dailey, H. A., and Fleming, J. E. (1986). The role of arginyl residues in porphyrin binding to ferrochelatase. J Biol Chem *261*, 7902-7905.

Dailey, H. A., Jones, C. S., and Karr, S. W. (1989). Interaction of free porphyrins and metalloporphyrins with mouse ferrochelatase. A model for the active site of ferrochelatase. Biochim Biophys Acta *999*, 7-11.

Dailey, H. A., Sellers, V. M., and Dailey, T. A. (1994b). Mammalian ferrochelatase. Expression and characterization of normal and two human protoporphyric ferrochelatases. J Biol Chem *269*, 390-395.

Dailey, T. A., and Dailey, H. A. (1996b). Human protoporphyrinogen oxidase: Expression, purification, and characterization of the cloned enzyme. Protein Sci *5*, 98-105.

Dailey, T. A., and Dailey, H. A. (2002). Identification of [2Fe-2S] clusters in microbial ferrochelatases. J Bacteriol *184*, 2460-2464.

Dailey, T. A., Dailey, H. A., Meissner, P., and Prasad, A. R. K. (1995). Cloning, sequence, and expression of mouse protoporphyrinogen oxidase. Arch Biochem Biophys *324*, 379-384.

Dailey, T. A., Meissner, P., and Dailey, H. A. (1994c). Expression of a cloned protoporphyrinogen oxidase. J Biol Chem *269*, 813-815.

Dailey, T. A., Woodruff, J. H., and Dailey, H. A. (2005). Examination of mitochondrial protein targeting of haem synthetic enzymes: *in vivo* identification of three functional haem-responsive motifs in 5-aminolaevulinate synthase. Biochem J *386*, 381-386.

Day, A. L., Parsons, B. M., and Dailey, H. A. (1998). Cloning and characterization of *Gallus* and *Xenopus* ferrochelatases: presence of the [2Fe-2S] cluster in nonmammalian ferrochelatase. Arch Biochem Biophys *359*, 160-169.

De Matteis, F., Gibbs, A. H., and Smith, A. G. (1980). Inhibition of protohaem ferro-lyase by N-substituted porphyrins. Structural requirements for the inhibitory effect. Biochem J *189*, 645-648.

de Verneuil, H., Sassa, S., and Kappas, A. (1983). Purification and properties of uroporphyrinogen decarboxylase from human erythrocytes. A single enzyme catalyzing the four sequential decarboxylations of uroporphyrinogens I and III. J Biol Chem *258*, 2454-2460.

Deybach, J.-C., Silva, V., Grandchamp, B., and Nordmann, Y. (1985). The mitochondrial location of protoporphyrinogen oxidase. Eur J Biochem *149*, 431-435.

Di Pierro, E., Brancaleoni, V., Moriondo, V., Besana, V., Cappellini, M.D. (2007). Co-existence of two functional mutations on the same allele of the human ferrochelatase gene in erythropoietic protoporphyria. Clin Genet *71*, 84-88.

Dombeck, T. A., and Satonik, R. C. (2005). The porphyrias. Emerg Med Clin North Amer *23*, 885-899.

Elder, G. H., and Evans, J. O. (1978). A radiochemical method for the measurement of coproporphyrinogen oxidase and the utilization of substrates other than coproporphyrinogen III by the enzyme from rat liver. Biochem J *169*, 205-214.

Elder, G. H., Evans, J. O., Jackson, J. R., and Jackson, A. H. (1978). Factors determining the sequence of oxidative decarboxylation of the 2-and 4-propionate substituents of coproporphyrinogen III by coproporphyrinogen III oxidase in rat liver. Biochem J *169*, 215-223.

Elder, G. H., and Worwood, M. (1998). Mutations in the hemochromatosis gene, porphyria cutanea tarda, and iron overload. Hepatology *27*, 289-291.

Erskine, P. T., Newbold, R., Brindley, A. A., Wood, S. P., Shoolingin-Jordan, P. M., Warren, M. J., and Cooper, J. B. (2001). The X-ray structure of yeast 5-aminolaevulinic acid dehydratase complexed with substrate and three inhibitors. J Mol Biol *312*, 133-141.

Erskine, P. T., Senior, N., Awan, S., Lambert, R., Lewis, G., Tickle, I. J., Sarwar, M., Spencer, P., Thomas, P., and Warren, M. J. (1997). X-ray structure of 5-aminolaevulinate dehydratase, a hybrid aldolase. Nat Struct Biol *4*, 1025-1031.

Falk, J. E. (1964). Porphyrins and Metalloporphyrins, Vol 2 (Amsterdam: Elsevier Publishing).

Faller, M., Matsunaga, M., Yin, S., Loo, J. A., and Guo, F. (2007). Heme is involved in microRNA processing. Nat Struct Mol Biol *14*, 23-29.

Ferreira, G. C. (1995). Heme biosynthesis: biochemistry, molecular biology, and relationship to disease. J Bioenerg Biomembr *27*, 147-150.

Ferreira, G. C., Andrew, T. L., Karr, S. W., and Dailey, H. A. (1988). Organization of the terminal two enzymes of the heme biosynthetic pathway. Orientation of protoporphyrinogen oxidase and evidence for a membrane complex. J Biol Chem *263*, 3835-3839.

Ferreira, G. C., Franco, R., Lloyd, S. G., Pereira, A. S., Moura, I., Moura, J. J., and Huynh, B. H. (1994). Mammalian ferrochelatase, a new addition to the metalloenzyme family. J Biol Chem *269*, 7062-7065.

Frustaci, J. M., and O'Brian, M. R. (1993). The *Escherichia coli* visA gene encodes ferrochelatase, the final enzyme of the heme biosynthetic pathway. J Bacteriol *175*, 2154-2156.

Funk, C., and Vermaas, W. (1999). A cyanobacterial gene family coding for single-helix proteins resembling part of the light-harvesting proteins from higher plants. Biochemistry *38*, 9397-9404.

Garrett, R. H., and Grisham, C. M. (1999). Biochemistry, 2nd edn (Fort Worth: Saunders College Publishing).

Ghisla, S., and Massey, V. (1989). Mechanisms of flavoprotein-catalyzed reactions. FEBS J *181*, 1-17.

Goldberg, A., Ashenrucker, M., Cartwright, G. E., and Wintrobe, M. M. (1956). Studies on the biosynthesis of heme *in vitro* by avian erythrocytes. Blood *11*, 821-833.

Goldberg, D. E., and Thomas, K. M. (1976). Crystal and molecular structure of an N-substituted porphyrin, chloro (2, 3, 7, 8, 12, 13, 17, 18-octaethyl-N-ethylacetatoporphine) cobalt (II). J Am Chem Soc *98*, 913-919.

Gollub, E. G., Liu, K. P., Dayan, J., Adlersberg, M., and Sprinson, D. B. (1977). Yeast mutants deficient in heme biosynthesis and a heme mutant additionally blocked in cyclization of 2,3-oxidosqualene. J Biol Chem *252*, 2846-2854.

Gora, M., Grzybowska, E., Rytka, J., and Labbe-Bois, R. (1996). Probing the active-site residues in *Saccharomyces cerevisiae* ferrochelatase by directed mutagenesis. In vivo and in vitro analyses. J Biol Chem *271*, 11810-11816.

Gough, S. P., and Kannangara, C. G. (1977). Synthesis of 6-aminolevulinate by a chloroplast stroma preparation from greening barley leaves. Carlsberg Res Commun *42*, 459-464.

Gouya, L., Deybach, J. C., Lamoril, J., Da Silva, V., Beaumont, C., Grandchamp, B., and Nordmann, Y. (1996). Modulation of the phenotype in dominant erythropoietic protoporphyria by a low expression of the normal ferrochelatase allele. Am J Hum Genet *58*, 292-299.

Gouya, L., Martin-Schmitt, C., Robreau, A.-M., Austerlitz, F., Da Silva, V., Brun, P., Simonin, S., Lyoumi, S., Grandchamp, B., Beaumont, C., *et al.* (2006). Contribution of a common single-nucleotide polymorphism to the genetic predisposition for erythropoietic protoporphyria. Am J Hum Genet *78*, 2-14.

Gouya, L., Puy, H., Lamoril, J., Da Silva, V., Grandchamp, B., Nordmann, Y., and Deybach, J. C. (1999). Inheritance in erythropoietic protoporphyria: a common wild-type ferrochelatase allelic variant with low expression accounts for clinical manifestation. Blood *93*, 2105-2110.

Grandchamp, B., Phung, N., and Nordmann, Y. (1978). The mitochondrial localization of coproporphyrinogen III oxidase. Biochem J *176*, 102.

Grimm, B. (2003). Regulatory mechanisms of eukaryotic tetrapyrrole biosynthesis, In The Porphyrin Handbook, K. M. Kadish, Smith, K.M., and Guilard, R., ed. (San Diego: Academic Press), pp. 1-32.

Hambright, P. (1975). Dynamic coordination chemistry of metalloporphyrins, In Porphyrins and Metalloporphyrins, K. Smith, ed. (Amsterdam: Elsevier), pp. 233–278.

Hansson, M., Gough, S. P., Kannangara, C. G., and von Wettstein, D. (1998). Chromosomal locations of six barley genes encoding enzymes of chlorophyll and heme biosynthesis and the sequence of the ferrochelatase gene identify two regulatory genes. Plant Physiol Biochem *36*, 545-554.

Hansson, M., and Hederstedt, L. (1992). Cloning and characterization of the *Bacillus subtilis* hemEHY gene cluster, which encodes protoheme IX biosynthetic enzymes. J Bacteriol *174*, 8081-8093.

Harbin, B. M., and Dailey, H. A. (1985). Orientation of ferrochelatase in bovine liver mitochondria. Biochemistry *24*, 366-370.

Hart, G. J., Miller, A. D., and Battersby, A. R. (1988). Evidence that the pyrromethane cofactor of hydroxymethylbilane synthase (porphobilinogen deaminase) is bound through the sulphur atom of a cysteine residue. Biochem J *252*, 909-912.

Honeybourne, C. L., Jackson, J. T., and Jones, O. T. (1979). The interaction of mitochondrial ferrochelatase with a range of porphyrin substrates. FEBS Lett *98*, 207-210.

Jackson, A. H., Sancovich, H. A., Ferramola, A. M., Evans, N., Games, D. E., and Matlin, S. A. (1976). Macrocyclic intermediates in the biosynthesis of porphyrins. Philos Trans R Soc Lond B Biol Sci *273*, 191-206.

Jaffe, E. K. (1995). Porphobilinogen synthase, the first source of heme's asymmetry. J Bioenerg Biomembr *27*, 169-179.

Jaffe, E. K., Bagla, S., and Michini, P. A. (1991). Reevaluation of a sensitive indicator of early lead exposure. Measurement of porphobilinogen synthase in blood. Biol Trace Elem Res *28*, 223-231.

Jinli, L. U. O., and Lim, C. K. (1993). Order of uroporphyrinogen III decarboxylation on incubation of porphobilinogen and uroporphyrinogen III with erythrocyte uroporphyrinogen decarboxylase. Biochem J *289*, 529-532.

Jones, M. S., and Jones, O. T. (1969). The structural organization of haem synthesis in rat liver mitochondria. Biochem J *113*, 507-514.

Jordan, P. M. (1990). Biosynthesis of 5-aminolevulinic acid and its transformation into coproporphyrinogen in animals and bacteria, In Biosynthesis of Heme and Chlorophylls (New York: McGraw-Hill), pp. 55-122.

Jordan, P. M. (1991a). Biosynthesis of tetrapyrroles, In Biosynthesis of Tetrapyrroles, P. M. Jordan, ed. (Amsterdam ; New York: Elsevier), pp. xii, 309.

Jordan, P. M. (1991b). Biosynthesis of tetrapyrroles, In New Comprehensive Biochemistry, P. M. Jordan, ed. (New York: Elsevier), pp. 1-66.

Jordan, P. M., and Warren, M. J. (1987). Evidence for a dipyrromethane cofactor at the catalytic site of *E. coli* porphobilinogen deaminase. FEBS Lett *225*, 87-92.

Kannangara, C. G., and Gough, S. P. (1979). Biosynthesis of d-aminolevulinate in greening barley leaves. II. Induction of enzyme synthesis by light. Carlsberg Res Commun *44*, 11-20.

Kappas, A., Sassa, S., and Galbraith, R. A. (1995). The Porphyrias, In The Metabolic and Molecular Basis of Inherited Disease, C. R. Scriver, Beaudet, A.L., Sly, W.S., Valle, D., ed. (New York: McGraw-Hill, Inc.), pp. 2103-2159.

Karlberg, T., Lecerof, D., Gora, M., Silvegren, G., Labbe-Bois, R., Hansson, M., and Al-Karadaghi, S. (2002). Metal binding to *Saccharomyces cerevisiae* ferrochelatase. Biochemistry *41*, 13499-13506.

Karr, S. R., and Dailey, H. A. (1988). The synthesis of murine ferrochelatase *in vitro* and *in vivo*. Biochem J *254*, 799-803.

Kauppinen, R. (2005). Porphyrias. Lancet *365*, 241-252.

Koch, M., Breithaupt, C., Kiefersauer, R., Freigang, J. r., Huber, R., and Messerschmidt, A. (2004). Crystal structure of protoporphyrinogen IX oxidase: a key enzyme in haem and chlorophyll biosynthesis. EMBO J *23*, 1720-1728.

Labbe-Bois, R. (1990). The ferrochelatase from *Saccharomyces cerevisiae*. Sequence, disruption, and expression of its structural gene *HEM15*. J Biol Chem *265*, 7278-7283.

Lash, T. D. (1991). Action of uroporphyrinogen decarboxylase on uroporphyrinogen-III: a reassessment of the clockwise decarboxylation hypothesis. Biochem J *278*, 901-903.

Lavallee, D. K. (1987). The chemistry and biochemistry of N-substituted porphyrins (New York: VCH Publishers).

Lavallee, D. K. (1988). Mechanistic principles of enzyme activity, In, J. F. Liebman, and A. Greenberg, eds. (New York: VCH Publishers), pp. 279-314.

Layer, G., Moser, J., Heinz, D. W., Jahn, D., and Schubert, W. D. (2003). Crystal structure of coproporphyrinogen III oxidase reveals cofactor geometry of Radical SAM enzymes. EMBO J *22*, 6214-6224.

Lecerof, D., Fodje, M., Hansson, A., Hansson, M., and Al-Karadaghi, S. (2000). Structural and mechanistic basis of porphyrin metallation by ferrochelatase. J Mol Biol *297*, 221-232.

Lee, D. S., Flachsová, E., Bodnárová, M., Demeler, B., Martásek, P., and Raman, C. S. (2005). Structural basis of hereditary coproporphyria. Proc Natl Acad Sci USA *102*, 14232-14237.

Lermontova, I., Kruse, E., Mock, H. P., and Grimm, B. (1997). Cloning and characterization of a plastidal and a mitochondrial isoform of tobacco protoporphyrinogen IX oxidase. Proc Natl Acad Sci USA *94*, 8895-8900.

Li, Y., and Sen, D. (1996). A catalytic DNA for porphyrin metallation. Nat Struct Biol *3*, 743-747.

Little, H. N., Jones, O.T.G. (1976). The subcellular localization and properties of the ferrochelatase of etiolated barley. Biochem J *156*, 309–314.

Louie, G. V., Brownlie, P. D., and Lambert, R. (1996). The three-dimensional structure of *Escherichia coli* porphobilinogen deaminase at 1.76-A resolution. Proteins *25*, 48-78.

Louie, G. V., Brownlie, P. D., Lambert, R., Cooper, J. B., Blundell, T. L., Wood, S. P., Warren, M. J., Woodcock, S. C., and Jordan, P. M. (1992). Structure of porphobilinogen deaminase reveals a flexible multidomain polymerase with a single catalytic site. Nature *359*, 33-39.

Magness, S. T., Tugores, A., and Brenner, D. A. (2000). Analysis of ferrochelatase expression during hematopoietic development of embryonic stem cells. Blood *95*, 3568-3577.

Magnus, I. A., Jarrett, A., Prankerd, T. A., and Rimington, C. (1961). Erythropoietic protoporphyria. A new porphyria syndrome with solar urticaria due to protoporphyrinaemia. Lancet *2*, 448-451.

Marks, G. S. (1987). Interaction of chemicals with hemoproteins: implications for the mechanism of action of porphyrinogenic drugs and nitroglycerin. Can J Physiol Pharmacol *65*, 1111-1119.

Marks, G. S., Allen, D. T., Johnston, C. T., Sutherland, E. P., Nakatsu, K., and Whitney, R. A. (1985). Suicidal destruction of cytochrome P-450 and reduction of ferrochelatase activity by 3, 5-diethoxycarbonyl-1, 4-dihydro-2, 4, 6-trimethylpyridine and its analogues in chick embryo liver cells. Mol Pharmacol *27*, 459-465.

Martasek, P., Camadro, J. M., Raman, C. S., Lecomte, M. C., Le Caer, J. P., Demeler, B., Grandchamp, B., and Labbe, P. (1997). Human coproporphyrinogen oxidase. Biochemical characterization of recombinant normal and R231W mutated enzymes expressed in *E. coli* as soluble, catalytically active homodimers. Cell Mol Biol (Noisy-le-grand) *43*, 47-58.

Martins, B. M., Grimm, B., Mock, H. P., Huber, R., and Messerschmidt, A. (2001). Crystal structure and substrate binding modeling of the uroporphyrinogen-III decarboxylase from *Nicotiana tabacum*. Implications for the catalytic mechanism. J Biol Chem *276*, 44108-44116.

Mascaro, J. M., ed. (1986). The Porphyrias. Semin Dermat *5*, 69-212.

Mathews-Roth, M. M., Pathak, M. A., Fitzpatrick, T. B., Harber, L. H., and Kass, E. H. (1977). Beta carotene therapy for erythropoietic protoporphyria and other photosensitivity diseases. Arch Dermatol *113*, 1229-1232.

Mathews, M. A. A., Schubert, H. L., Whitby, F. G., Alexander, K. J., Schadick, K., Bergonia, H. A., Phillips, J. D., and Hill, C. P. (2001). Crystal structure of human uroporphyrinogen III synthase. EMBO J *20*, 5832-5839.

Mathewson, J. H., and Corwin, A. H. (1961). Biosynthesis of pyrrole pigments: A mechanism for porphobilinogen polymerization1. J Am Chem Soc *83*, 135-137.

Matringe, M., Camadro, J. M., Labbe, P., and Scalla, R. (1989). Protoporphyrinogen oxidase as a molecular target for diphenyl ether herbicides. Biochem J *260*, 231-235.

Medlock, A. E. (2000) The terminal enzymes of the heme biosynthetic pathway: enzymology and transgenic studies, Thesis Ph D --University of Georgia 2000.

Medlock, A. E., and Dailey, H. A. (2000). Examination of the activity of carboxyl-terminal chimeric constructs of human and yeast ferrochelatases. Biochemistry *39*, 7461-7467.

Medlock, A. E., and Dailey, H. A. (2004). Human coproporphyrinogen oxidase is not a metalloprotein. J Biol Chem *279*, 38960-38968.

Medlock, A. E., Swartz, L., Dailey, T. A., Dailey, H. A., and Lanzilotta, W. N. (2007). Substrate interactions with human ferrochelatase. Proc Natl Acad Sci USA *104*, 1789-1793.

Mense, S. M., and Zhang, L. (2006). Heme: a versatile signaling molecule controlling the activities of diverse regulators ranging from transcription factors to MAP kinases. Cell Res *16*, 681-692.

Miyamoto, K., Nakahigashi, K., Nishimura, K., and Inokuchi, H. (1991). Isolation and characterization of visible light-sensitive mutants of *Escherichia coli* K12. J Mol Biol *219*, 393-398.

Moore M, M. K., Fitzsimons E, Goldberg S. (1990). The porphyrias. Blood Rev *4*, 88-96.

Moore, M. R. (1993). Biochemistry of porphyria. Int J Biochem *25*, 1353-1368.

Moore, M. R., and Wintrobe, M. M. (1987). Disorders of Porphyrin Metabolism, Vol 1 (New York: Plenum Medical).

Moulin, M., and Smith, A. G. (2005). Regulation of tetrapyrrole biosynthesis in higher plants. Biochem Soc Trans *33*, 737-742.

Muhlenhoff, U., Stadler, J. A., Richhardt, N., Seubert, A., Eickhorst, T., Schweyen, R. J., Lill, R., and Wiesenberger, G. (2003). A specific role of the yeast mitochondrial carriers MRS3/4p in mitochondrial iron acquisition under iron-limiting conditions. J Biol Chem *278*, 40612-40620.

Najahi-Missaoui, W., and Dailey, H. A. (2005). Production and characterization of erythropoietic protoporphyric heterodimeric ferrochelatases. Blood *106*, 1098-1104.

Nakahashi, Y., Taketani, S., Okuda, M., Inoue, K., and Tokunaga, R. (1990). Molecular cloning and sequence analysis of cDNA encoding human ferrochelatase. Biochem Biophys Res Comm *173*, 748-755.

Nakahigashi, K., Nishimura, K., Miyamoto, K., and Inokuchi, H. (1991). Photosensitivity of a protoporphyrin-accumulating, light-sensitive mutant (*visA*) of *Escherichia coli* K-12. Proc Natl Acad Sci USA *88*, 10520-10524.

Napier, I., Ponka, P., and Richardson, D. R. (2005). Iron trafficking in the mitochondrion: novel pathways revealed by disease. Blood *105*, 1867-1874.

Oborník, M., and Green, B. R. (2005). Mosaic origin of the heme biosynthesis pathway in photosynthetic eukaryotes. Mol Biol Evol *22*, 2343-2353.

Olsson, U., Billberg, A., Sjovall, S., Al-Karadaghi, S., and Hansson, M. (2002). In vivo and in vitro studies of *Bacillus subtilis* ferrochelatase mutants suggest substrate channeling in the heme biosynthesis pathway. J Bacteriol *184*, 4018-4024.

Ostasiewicz, L. T., Huang, J. L., Wang, X., Piomelli, S., and Poh-Fitzpatrick, M. B. (1995). Human protoporphyria: genetic heterogeneity at the ferrochelatase locus. Photodermatol Photoimmunol Photomed *11*, 18-21.

Phillips, J. D., Whitby, F. G., Kushner, J. P., and Hill, C. P. (1997). Characterization and crystallization of human uroporphyrinogen decarboxylase. Prot Sci *6*, 1343.

Phillips, J. D., Whitby, F. G., Warby, C. A., Labbe, P., Yang, C., Pflugrath, J. W., Ferrara, J. D., Robinson, H., Kushner, J. P., and Hill, C. P. (2004). Crystal structure of the

oxygen-dependant coproporphyrinogen oxidase (Hem13p) of *Saccharomyces cerevisiae*. J Biol Chem *279*, 38960.

Poh-Fitzpatrick, M. B. (1984). Diagnosis and treatment of erythropoietic protoporphyria. Compr Ther *10*, 12-17.

Poh-Fitzpatrick, M. B. (1985). Porphyrin-sensitized cutaneous photosensitivity: pathogenesis and treatment. Clin Dermatol *3*, 41-82.

Ponka, P. (1997). Tissue-specific regulation of iron metabolism and heme synthesis: distinct control mechanisms in erythroid cells. Blood *89*, 1-25.

Poulson, R., and Polglase, W. J. (1975). The enzymic conversion of protoporphyrinogen IX to protoporphyrin IX. Protoporphyrinogen oxidase activity in mitochondrial extracts of *Saccharomyces cerevisiae*. J Biol Chem *250*, 1269-1274.

Prasad, A. R., and Dailey, H. A. (1995). Effect of cellular location on the function of ferrochelatase. J Biol Chem *270*, 18198-18200.

Proulx, K. L., and Dailey, H. A. (1992). Characteristics of murine protoporphyrinogen oxidase. Protein Sci *1*, 801-809.

Romeo, P. H., Raich, N., Dubart, A., Beaupain, D., Pryor, M., Kushner, J., Cohen-Solal, M., and Goossens, M. (1986). Molecular cloning and nucleotide sequence of a complete human uroporphyrinogen decarboxylase cDNA. J Biol Chem *261*, 9825-9831.

Sassa, S. (2006). Modern diagnosis and management of the porphyrias. Br J Haematol *135*, 281-292.

Schneider-Yin, X., Gouya, L., Meier-Weinand, A., Deybach, J. C., and Minder, E. I. (2000). New insights into the pathogenesis of erythropoietic protoporphyria and their impact on patient care. Eur J Pediatr *159*, 719-725.

Schneider-Yin, X., Rufenacht, U. B., Hergersberg, M., Schnyder, C., Deybach, J. C., and Minder, E. I. (2001). Haplotype analysis in determination of the heredity of erythropoietic protoporphyria among Swiss families. Journal Invest Dermatol *117*, 1521-1525.

Scholnick, P., Marver, H. S., and Schmid, R. (1971). Erythropoietic protoporphyria: evidence for multiple sites of excess protoporphyrin formation. J Clin Invest *50*, 203-207.

Scriver, C. R. (1989). The Metabolic Basis of Inherited Disease (New York: McGraw-Hill).

Sellers, V. M., Dailey, T. A., and Dailey, H. A. (1998a). Examination of ferrochelatase mutations that cause erythropoietic protoporphyria. Blood *91*, 3980-3985.

Sellers, V. M., Wang, K. F., Johnson, M. K., and Dailey, H. A. (1998b). Evidence that the fourth ligand to the [2Fe-2S] cluster in animal ferrochelatase is a cysteine. Characterization of the enzyme from *Drosophila melanogaster*. J Biol Chem *273*, 22311-22316.

Sellers, V. M., Wu, C. K., Dailey, T. A., and Dailey, H. A. (2001). Human ferrochelatase: characterization of substrate-iron binding and proton-abstracting residues. Biochemistry *40*, 9821-9827.

Shaw, G. C., Cope, J. J., Li, L., Corson, K., Hersey, C., Ackermann, G. E., Gwynn, B., Lambert, A. J., Wingert, R. A., Traver, D.*, et al.* (2006). Mitoferrin is essential for erythroid iron assimilation. Nature *440*, 96-100.

Shepherd, M., Dailey, T. A., and Dailey, H. A. (2006). A new class of [2Fe-2S]-cluster-containing protoporphyrin (IX) ferrochelatases. Biochem J *397*, 47-52.

Shibuya, H., Nonneman, D., Tamassia, M., Allphin, O. L., and Johnson, G. S. (1995). The coding sequence of the bovine ferrochelatase gene. Biochim Biophys Acta *1231*, 117-120.

Shoolingin-Jordan, P. M. (2003). The Biosynthesis of Coproporphyrinogen III, In The Porphyrin Handbook, K. M. Kadish, Smith, K.M., Guillard, R., ed. (USA: Elsevier Science), pp. 33-74.

Sofia, H. J., Chen, G., Hetzler, B. G., Reyes-Spindola, J. F., and Miller, N. E. (2001). Radical SAM, a novel protein superfamily linking unresolved steps in familiar biosynthetic pathways with radical mechanisms: functional characterization using new analysis and information visualization methods. Nucleic Acids Res *29*, 1097-1106.

Solis, C., Martinez-Bermejo, A., Naidich, T. P., Kaufmann, W. E., Astrin, K. H., Bishop, D. F., and Desnick, R. J. (2004). Acute intermittent porphyria studies of the severe homozygous dominant disease provides insights into the neurologic attacks in acute porphyrias. Arch Neurol *61*, 1764-1770.

Soonawalla, Z. F., Orug, T., Badminton, M. N., Elder, G. H., Rhodes, J. M., Bramhall, S. R., and Elias, E. (2004). Liver transplantation as a cure for acute intermittent porphyria. Lancet *363*, 705-706.

Stanbury, J. B., Wyngaarden, J.G., Fredrickson, D.S., Goldstein, J.L., and Brown, M.S. (1983). Disorders of porphyrin and heme metabolism, In The Metabolic Basis of Inherited Disease (New York: McGraw-Hill), pp. 1322-1325.

Straka, J. G., and Kushner, J. P. (1983). Purification and characterization of bovine hepatic uroporphyrinogen decarboxylase. Biochemistry *22*, 4664-4672.

Suzuki, T., Masuda, T., Inokuchi, H., Shimada, H., Ohta, H., and Takamiya, K. (2000). Overexpression, enzymatic properties and tissue localization of a ferrochelatase of cucumber. Plant Cell Physiol *41*, 192-199.

Suzuki, T., Masuda, T., Singh, D. P., Tan, F. C., Tsuchiya, T., Shimada, H., Ohta, H., Smith, A. G., and Takamiya, K. (2002). Two types of ferrochelatase in photosynthetic and nonphotosynthetic tissues of cucumber. Their difference in phylogeny, gene expression, and localization. J Biol Chem *277*, 4731-4737.

Takeda, J., Ohya, T., and Sato, M. (1992). A ferrochelatase transition-state model. Rapid incorporation of copper (II) into nonplanar dodecaphenylporphyrin. Inorg Chem *31*, 2877-2880.

Taketani, S., Nakahashi, Y., Osumi, T., and Tokunaga, R. (1990). Molecular cloning, sequencing, and expression of mouse ferrochelatase. J Biol Chem *265*, 19377-19380.

Todd, D. J. (1998). Molecular genetics of erythropoietic protoporphyria. Photodermatol Photoimmunol Photomed *14*, 70-73.

Voet, J. G., and Voet, D. (2004). Biochemistry, 3rd edn (New York: J. Wiley & Sons).

Wang, K.-F., Dailey, T. A., and Dailey, H. A. (2001). Expression and characterization of the terminal heme synthetic enzymes from the hyperthermophile *Aquifex aeolicus*. Microbiol Lett *202*, 115-119.

Wang, W. Y., Huang, D. D., Stachon, D., Gough, S. P., and Kannangara, C. G. (1984). Purification, characterization, and fractionation of the d-aminolevulinic acid synthesizing enzymes from light-grown *Chlamydomonas reinhardtii* cells 1. Plant Physiol *74*, 569-575.

Warren, M. J., and Jordan, P. M. (1988). Investigation into the nature of substrate binding to the dipyrromethane cofactor of *Escherichia coli* porphobilinogen deaminase. Biochemistry *27*, 9020-9030.

Weinstein, J. D., and Beale, S. I. (1985). RNA is required for enzymatic conversion of glutamate to delta-aminolevulinate by extracts of *Chlorella vulgaris*. Arch Biochem Biophys *239*, 87-93.

Welsh, M. J., Tsui, L. C., Boat, T. F., and Beaudet, A. L. (1995). Cystic Fibrosis, In The Metabolic and Molecular Basis of Inherited Disease
A. L. Beaudet, Sly, W.S., and Valle, D., ed. (New York: McGraw-Hill, Inc), pp. 3799-3876.

Whitcombe, D. M., Carter, N. P., Albertson, D. G., Smith, S. J., Rhodes, D. A., and Cox, T. M. (1991). Assignment of the human ferrochelatase gene (FECH) and a locus for protoporphyria to chromosome 18q22. Genomics *11*, 1152-1154.

Wu, C. K., Dailey, H. A., Rose, J. P., Burden, A., Sellers, V. M., and Wang, B. C. (2001). The 2.0 A structure of human ferrochelatase, the terminal enzyme of heme biosynthesis. Nat Struct Biol *8*, 156-160.

Yoshinaga, T., and Sano, S. (1980). Coproporphyrinogen oxidase I. Purification, properties, and activation by phospholipids. J Biol Chem *255*, 4722-4726.

Zhang, Y., Lyver, E. R., Knight, S. A. B., Lesuisse, E., and Dancis, A. (2005). Frataxin and mitochondrial carrier proteins, Mrs3p and Mrs4p, cooperate in providing iron for heme synthesis. J Biol Chem *280*, 19794-19807.

Figure 1-1. The heme biosynthetic pathway. ALA: aminolevulinic acid; PBG: porphobilinogen (Medlock, 2000).

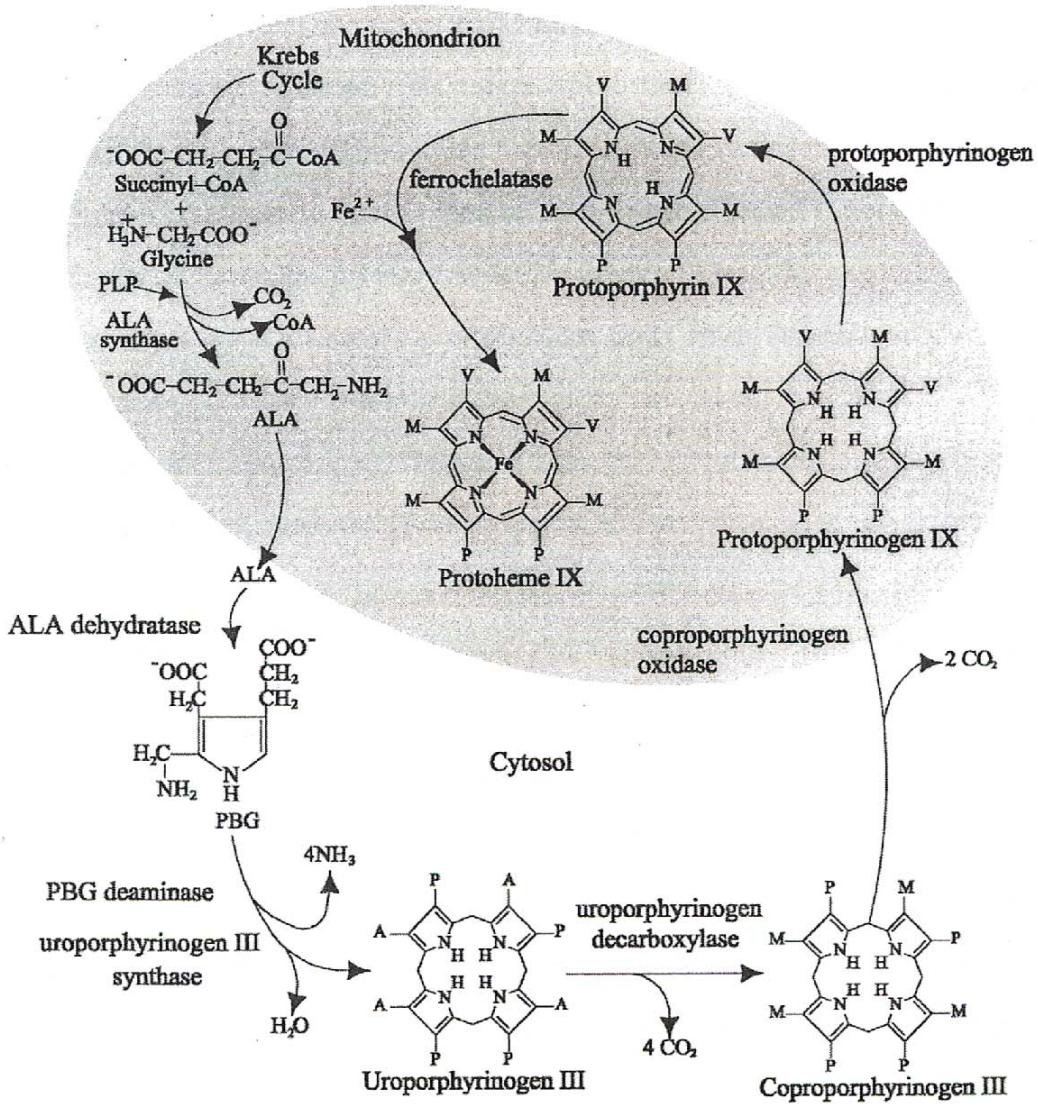
Mitochondrion
Krebs Cycle
Succinyl–CoA
Glycine
PLP
ALA synthase
CO2
CoA
ALA
ferrochelatase
Fe2+
Protoporphyrin IX
protoporphyrinogen oxidase
Protoheme IX
Protoporphyrinogen IX
ALA dehydratase
PBG
coproporphyrinogen oxidase
2 CO2
Cytosol
4NH3
PBG deaminase
uroporphyrinogen III synthase
H2O
uroporphyrinogen decarboxylase
4 CO2
Uroporphyrinogen III
Coproporphyrinogen III

Figure 1-2. ALAD three-dimensional crystal structure: Monomer showing the extended N-terminal arm that is involved in dimerization. Zinc metal ions are shown as blue spheres. Image constructed using Pymol and PDB file 1AW5.

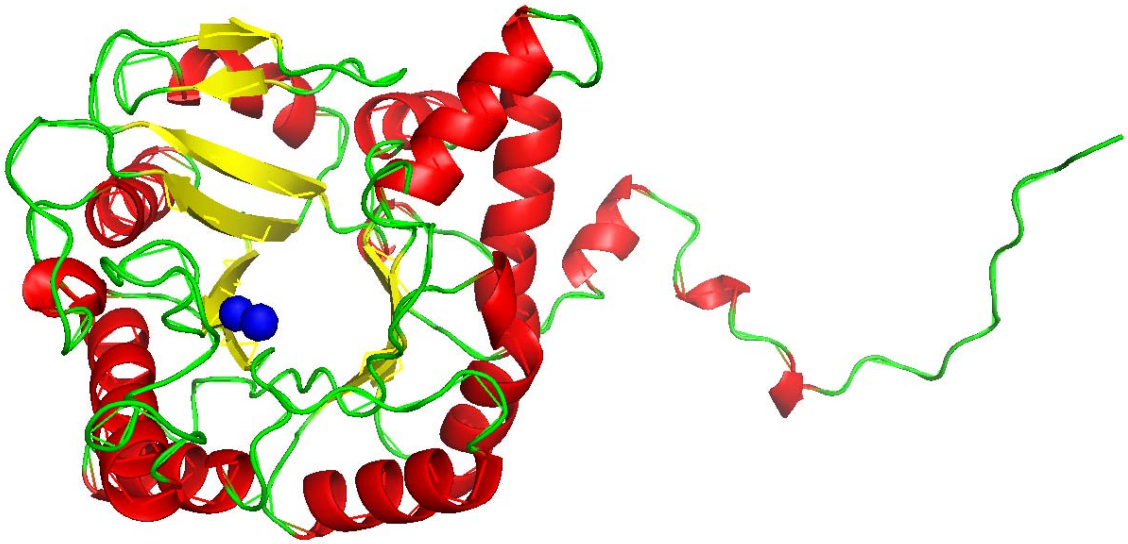

Fig 1-3. PBGD crystal structure. This figure shows the presence of three domains. Domain I (top left), domain II (top right), domain III (bottom). Also shown is the hydroxymethylbilane cofactor in red. Image constructed using Pymol and PDB code 1PDA.

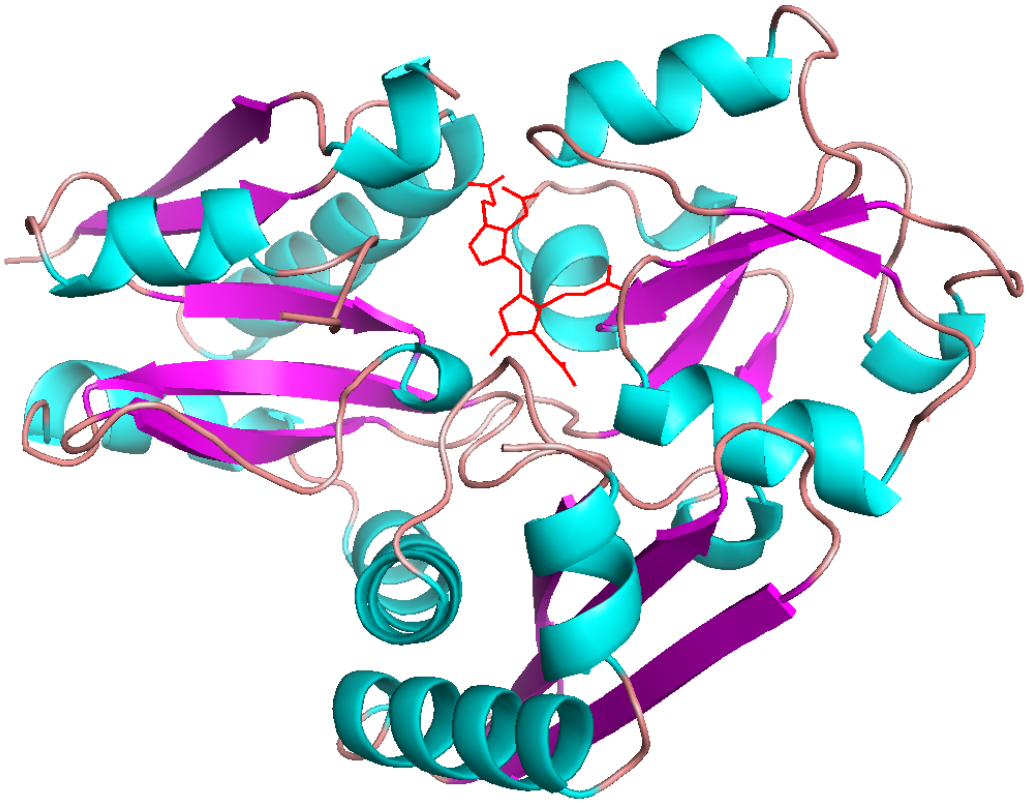

Fig 1-4. UROS structure. Domain I is shown in blue and is comprised of residues 1-35 and 173-260. Domain II is shown in red. Strands connecting the two domains are in yellow and are comprised of two anti-parallel β-sheets. The N-terminus is show in magenta. Image constructed using PyMol and PDB code 1JR2.

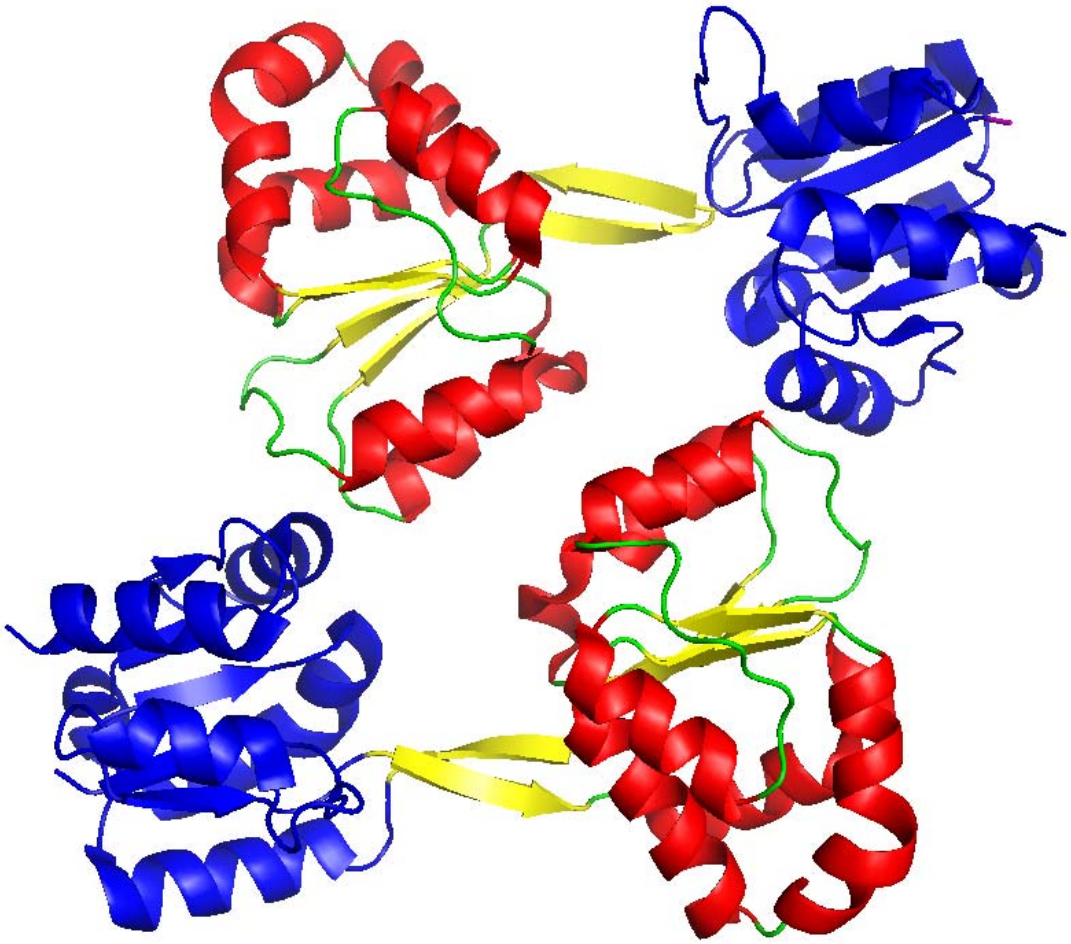

Fig 1-5. UROD crystal structure. This view is looking directly through the active site and shows in red some of the solvent-exposed residues that make up the active site. Image constructed using PyMol and PDB file 1URO.

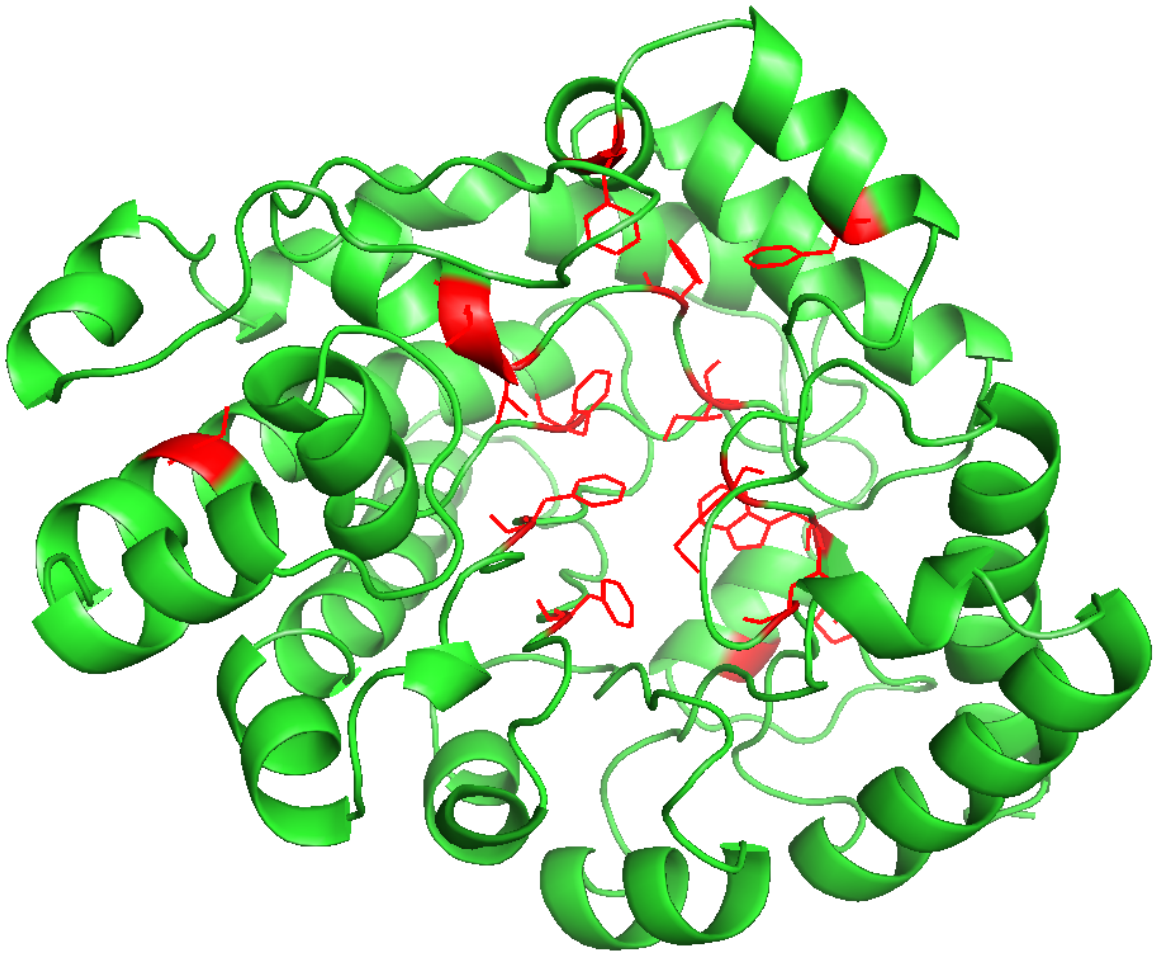

Fig 1-6. Yeast CPO monomer. The N-terminus is colored green. The active site is located between the β-sheets (raspberry) and the yellow α-helix. Image constructed using PyMol and PDB file 1TK1.

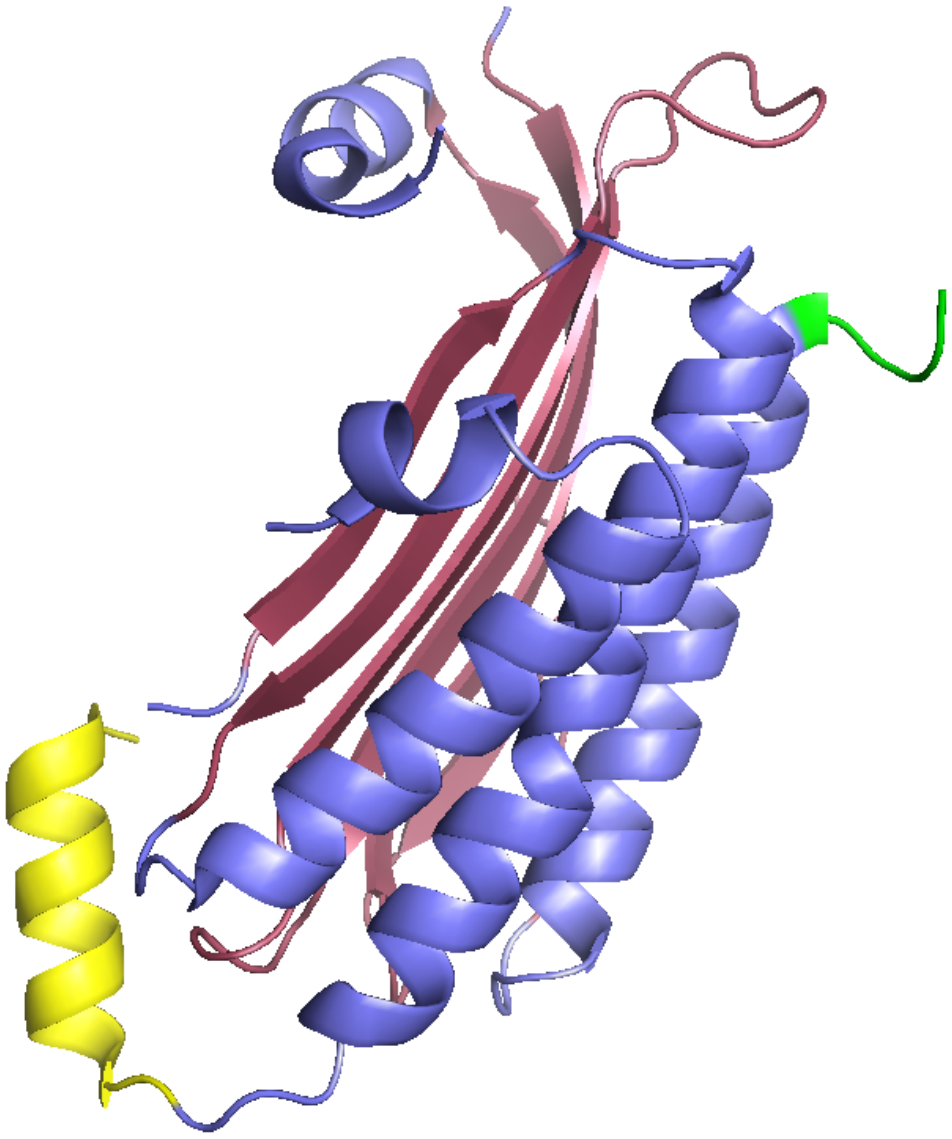

Fig 1-7. PPO2 dimer from tobacco. Yellow represents the membrane binding domain and cyan represents the substrate binding domain. The FAD molecules are shown as green sticks within the FAD-binding domain. Image generated using PyMol and PDB code 1SEZ.

Outer mitochondrial membrane

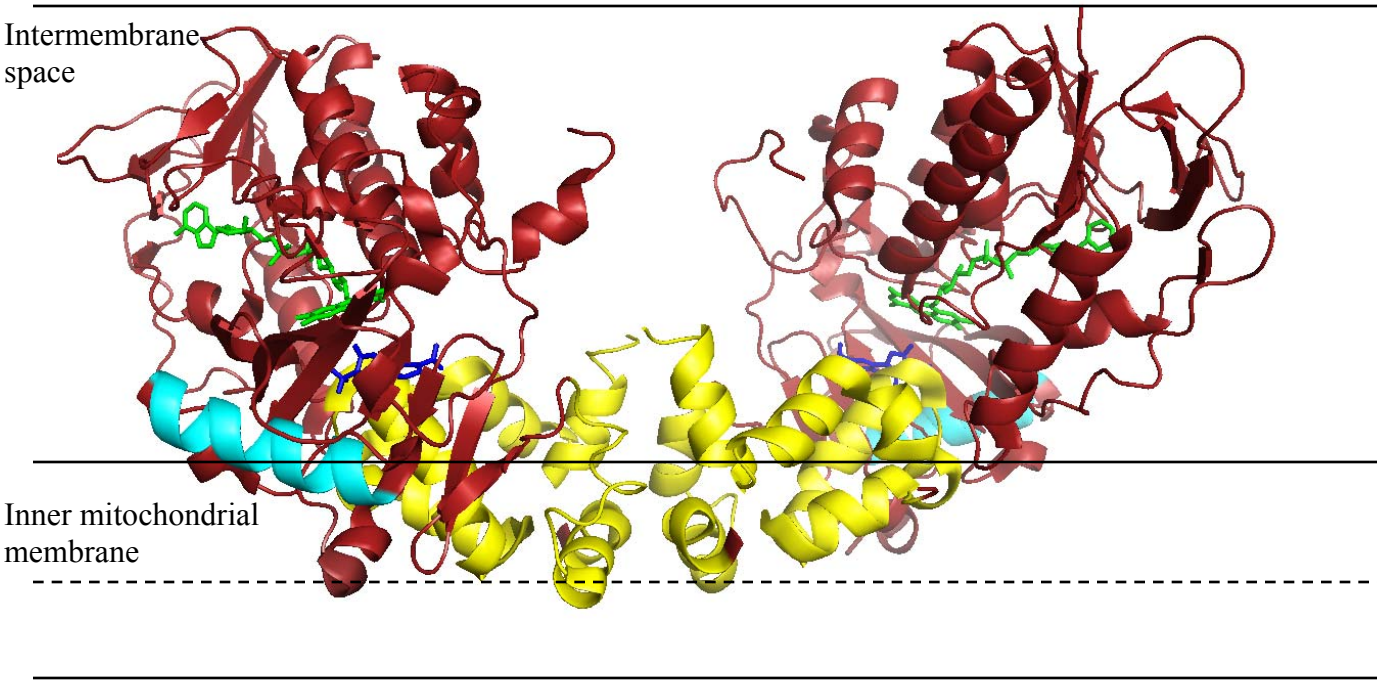

Mitochondrial matrix

Figure 1-8. Model showing the orientation and interaction of protoporphyrinogen oxidase (PPO) and ferrochelatase (Fc) for the transport of substrate protoporphyrin IX.

Intermembrane space

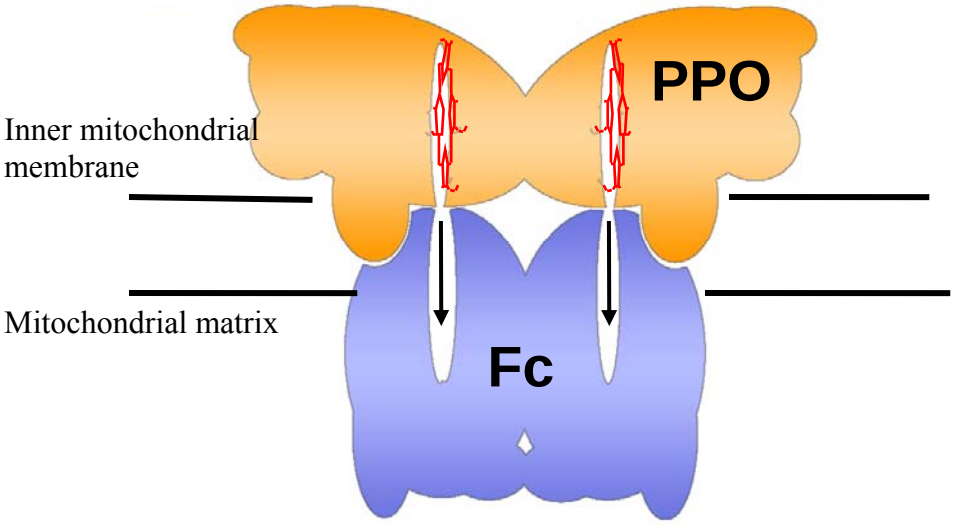

Figure 1-9. Reaction catalyzed by ferrochelatase (Dailey et al., 2000).

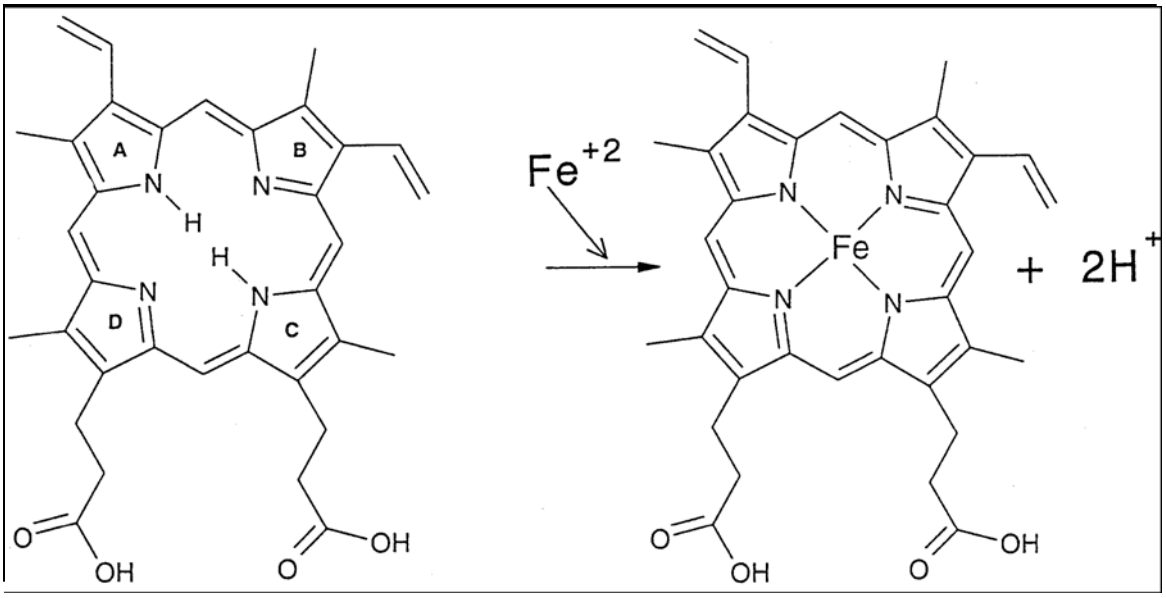
A
B
C
D
N
H
H
N
N
N
O
OH
O
OH
Fe+2
Fe
N
N
N
N
O
OH
O
OH
+ 2H+

Figure 1-10. Heme biosynthesis pathway in plants and non-plants. This figure shows the stepwise formation of ALA in plants (A) including the conversion of ALA to heme and chlorophyll. (B) Shows the direct incorporation of ALA from glycine and succinyl Co-A to form heme and cytochromes, which occurs in non-plant heme biosynthesis (Oborník and Green, 2005).

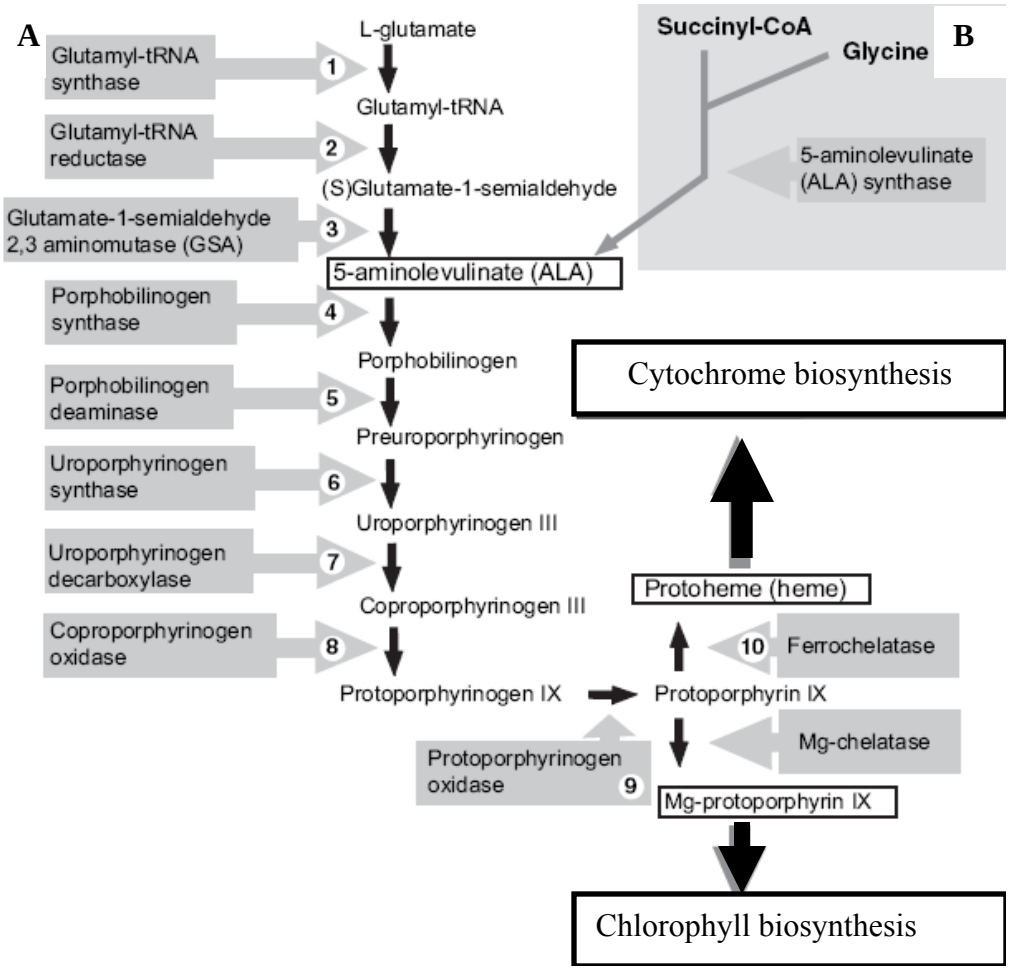
A
L-glutamate
Glutamyl-tRNA synthase
1
Glutamyl-tRNA
Glutamyl-tRNA reductase
2
(S)Glutamate-1-semialdehyde
Glutamate-1-semialdehyde 2,3 aminomutase (GSA)
3
5-aminolevulinate (ALA)
Porphobilinogen synthase
4
Porphobilinogen
Porphobilinogen deaminase
5
Preuroporphyrinogen
Uroporphyrinogen synthase
6
Uroporphyrinogen III
Uroporphyrinogen decarboxylase
7
Coproporphyrinogen III
Coproporphyrinogen oxidase
8
Protoporphyrinogen IX
Protoporphyrin IX
Protoporphyrinogen oxidase
9
10
Ferrochelatase
Protoheme (heme)
Mg-chelatase
Mg-protoporphyrin IX
Succinyl-CoA
Glycine
B
5-aminolevulinate (ALA) synthase
Cytochrome biosynthesis
Chlorophyll biosynthesis

Table 1-1. Porphyrias associated with the enzymes of the heme biosynthetic pathway. Adapted from Kauppinen, 2005.

Porphyria	**Enzyme defect**	**Inheritance**	**Site of heme precursor overproduction**	**Main clinical symptoms**
ALA-dehydratase deficient porphyria (Doss porphyria)	ALA dehydratase	Autosomal recessive	Liver	Acute attacks or chronic neuropathy
Acute intermittant porphyria (AIP)	Porphobilinogen deaminase	Autosomal dominant	Liver	Acute attacks
Congenital erythropoietic protoporphyria (CEP)	UroporphyrinogenIII synthase	Autosomal recessive	Erythroid cells	Severe photosensitivity and haemolysis
Porphyria cutanae tarda (PCT)	Uroporphyrinogen decarboxylase	Autosomal dominant or acquired	Liver	Skin fragility and chronic liver disease
Hereditary coproporphyria (HCP)	Coproporphyrinogen oxidase	Autosomal dominant	Liver	Acute attacks and skin fragility
Variegate porphyria (VP)	Protoporphyrinogen oxidase	Autosomal dominant	Liver	Acute attacks and skin fragility
Erythropoietic protoporphyria (EPP)	Ferrochelatase	Autosomal dominant	Erythroid cells	Photosensitivity and liver damage

Figure 1-11. Sequence homology of ferrochelatase from various species.

```
e_coli       ~~~~~~~~~~~~~~~~~~~~~~~~~~~~~~~~~~~~~~~~~~~~~~~~~~~~~~~~~~~~
m_xanthus    ~~~~~~~~~~~~~~~~~~~~~~~~~~~~~~~~~~~~~~~~~~~~~~~~~~~~~~~~~~~~
s_pombe      ~~~~~~~~~~~~~~~~~~~~~~~~~~~~~~~~~~~~MSVSSYSSDASSTVMDESPPNGVT
human        MRSLGANMAAALRAAGVLLRDPLASSSWRVCQPWRWKSGAAAAAVTTCTAQHAQGAKPQV
s_cerevesiae ~~~~~~~~~~~~~~~~~~~~~~~~~~~~~~MLSRTIRTQGSFLRRSQLTITRSFSVTFNM
c_crescentus ~~~~~~~~~~~~~~~~~~~~~~~~~~~~~~~~~~~~~~~~~~~~~~~~~~~~~~~~~~~~
b_subtilis   ~~~~~~~~~~~~~~~~~~~~~~~~~~~~~~~~~~~~~~~~~~~~~~~~~~~~~~~~~~~~
s_coelicolor ~~~~~~~~~~~~~~~~~~~~~~~~~~~~~~~~~~~~~~~~~~~~~~~~~~~~~~~~~~MP

e_coli       ~~~MRQTKTGILLANLGTPDAPTPEAVKRYLKQFLSDRRVVDTSRLLWWPLLRGVILPLR
m_xanthus    ~MPTPTSKRGLLLVNLGTPDAPQTGPVRRYLREFLNDPRVIDIHPLGRWALLNFIILPMR
s_pombe      KSVSGKGPTAVVMMNMGGPSNL..DEVGPFLERLFTDGDIIPL.GYFQNSLGKF.IAKRR
human        QPQKRKPKTGILMLNMGGPETL..GDVHDFLLRLFLDRDLMTL.P.IQNKLAPF.IAKRR
s_cerevesiae QNAQKRSPTGIVLMNMGGPSKV..EETYDFLYQLFADNDLIPISAKYQKTIAKY.IAKFR
c_crescentus ~~~~MTQKLAVVLFNLGGPDGP..DAVRPFLFNLFRDPAIIGAPALIRYPLAAL.ISTTR
b_subtilis   ~~~MSRKKMGLLVMAYGTPYKE..EDIERYYTHI...............RRGRK.PEPEM
s_coelicolor DVLDASPYDALLLLSFGGPEGP..DDVVPFLENV...............TRGRG.IPKER

e_coli       SPRVAKLYASVWMEGGSPLMVYSRQQQQALAQRL......P.EMPVALGMSYGSPSLESA
m_xanthus    PAKSAEAYRKIWMKEGSPLLVYSQALAAQVAERL......AGEYEVVLAMRYGSPSIPDG
s_pombe      TPKVQNHYSDI..GGGSPILHWTRIQGSEMCKILDKKCPESAPHLPFVAFRYAPPLTEDM
human        TPKIQEQYRRI..GGGSPIKIWTSKQGEGMVKLLDELSPNTAPHKYYIGFRYVHPLTEEA
s_cerevesiae TPKIEKQYREI..GGGSPIRKWSEYQATEVCKILDKTCPETAPHKPYVAFRYAKPLTAET
c_crescentus EKSAKANYAIM..GGGSPLLPETEKQARALEAALALAMPGVEA.KCFIAMRYWHPLTDET
b_subtilis   LQDLKDRYEAI..GGISPLAQITEQQAHNLEQHLNEIQDE.ITFKAYIGLKHIEPFIEDA
s_coelicolor LKEVGQHYFLF..GGVSP...INDQNRALLDALRKDFAEHGLDLPVYWGNRNWAPYLTDT

e_coli       VDELLAEHVDHIVVLPLYPQFSCSTVGAVWDELARIL....ARKRSIPGISFIRDYADNH
m_xanthus    IAALKARGVSEFTVLPLYPQEAASSTASSLARTYEVL....AQSWDVPFVRAVPAFFEHP
s_pombe      LDELKKANVSRAVAFSQYPQWSCATSGASLNELRRKLIEKGMEK..DFEWSIVDRWPLQQ
human        IEEMERDGLERAIAFTQYPQYSCSTTGSSLNAIYRYYNQVGRKP..TMKWSTIDRWPTHH
s_cerevesiae YKQMLKDGVKKAVAFSQYPHFSYSTTGSSINELWRQIKALDSER..SISWSVIDRWPTNE
c_crescentus ARQVAAFAPDQVVLLPLYPQFSTTTTGSSLKAWKKTYKGSGVQ.......TTVGCYPTEG
b_subtilis   VAEMHKDGITEAVSIVLAPHFSTFSVQSYNKR.....AKEEAEKLGGLTITSVESWYDEP
s_coelicolor LREMVGDGRRRILVLATSAYASYSGCRQYRENLADALAALESEGLELPKIDKLRHYFNHP

e_coli       DYINALANSVRASFAKHGEPD....LLLLSYHGIPQRYADEGD.................
m_xanthus    GFLDAF.TAVARPVIDDARAD....YVLFSFHGLPERHMRKSDPTGTHCLSTASCCDAMT
s_pombe      GLINAFAENIEETLKTYPEDVRDDVVIVFSAHSLPMSQVAK.......GD..PYVYE...
human        LLIQCFADHILKELDHFPLEKRSEVVILFSAHSLPMSVVNR.......GD..PYPQE...
s_cerevesiae GLIKAFSENITKKLQEFPQPVRDKVVLLFSAHSLPMDVVNT.......GD..AYPAE...
c_crescentus GLIEAHARMIRESWEKAGSP..TNIRLLFSAHGLPEKVILA.......GD..PYQKQ...
b_subtilis   KFVTYWVDRVKETYASMPEDERENAMLIVSAHSLPEK.......IKEFGD..PYPDQLHE
s_coelicolor GFVEPMVDGVVRSLAELPAEVRDGAHIAFCTHSIPTSAADGSGPVEEHGDGGAYVRQHLD

e_coli       DYPQRC.....RTTTRELASALGMAPEKVMMTFQSRFGRE..PWLMPYTDETLKMLGE.K
m_xanthus    DANRHCYRAQSYATARGLAQRLGLPAEGWSVSFQSRLGRT..PWVKPYTDVVLPELAK.K
s_pombe      .I.........AATSQAVMKRLNY.KNKFVNAWQSKVG.P.LPWMSPATDFVIEQLGN.R
human        .V.........SATVQKVMERLEY.CNPYRLVWQSKVG.P.MPWLGPQTDESIKGLCE.R
s_cerevesiae .V.........AATVYNIMQKLKF.KNPYRLVWQSQVG.P.KPWLGAQTAEIAEFLGP.K
c_crescentus .V.........EATAAAVAAHLPP.QIEWTVCYQSRVG.P.LKWIGPSTDDEIRRAGG.E
b_subtilis   SA.........KLIA....EGAGV.SE.YAVGWQSEGNTPD.PWLGPDVQDLTRDLFEQK
s_coelicolor VA.........RLIADAVRERTGV.DHPWQLVYQSRSGAPHIPWLEPDICDHLEER.QAA

e_coli       GVGHIQVMCPGFAADCLETLEEIAEQNREVFL.GAGGKKYEYIPALNATPEHIEMMANLV
m_xanthus    GVKRLAVMCPAFVADCLETLEEIGLRAREQFL.EAGGESLTLVPSLNAHPAWVDAVVRMV
s_pombe      GQKNMILVPIAFTSDHIETLKELE.DYIED.AKQKGITGVKRVSSINGSMTAIQGMADLV
human        GRKNILLVPIAFTSDHIETLYELDIEYSQVLAKECGVENIRRAESLNGNPLFSKALADLV
s_cerevesiae .VDGLMFIPIAFTSDHIETLHEIDLG...VIGESEYKDKFKRCESLNGNQTFIEGMADLV
c_crescentus D.KGVMITPIAFVSEHVETLVELDHEYAE.LAEEVGAAPYLRVSALGTAPEFIDGLAKAV
b_subtilis   GYQAFVYVPVGFVADHLEVLYDNDYE.CKVVTDDIGA.SYYRPEMPNAKPEFIDALATVV
s_coelicolor GVPAVVMAPIGFVSDHMEVLYDLDTE.ATAKAEELGL.PVRRSATVGADPRFAAAVRDLV
```

```
e_coli        AAYR~~~~~~~~~~~~~~~~~~~~~~~~~~~~~~~~~~~~~~~~~~~~~~
m_xanthus     RESDGPPTAVAGPLASAREPIPPR*~~~~~~~~~~~~~~~~~~~~~~~~~
s_pombe       AEHL.KAKVPYSRQFTQR.CPGCTSESCAERINFFQDF~~~~~~~~~~~~
human         HSHI.QSNELCSKQLTLS.CPLCVNPVCRETKSFFTSQQL~~~~~~~~~~
s_cerevesiae  KSHL.QSNQLYSNQLPLDFALGKSNDPVKDLSLVFGNHEST~~~~~~~~~
c_crescentus  RDSVGKAPGTVSSACGWRCGADWSKCPCREGASA~~~~~~~~~~~~~~~~
b_subtilis    LKKLGR~~~~~~~~~~~~~~~~~~~~~~~~~~~~~~~~~~~~~~~~~~~~
s_coelicolor  LERAGDERGQEVTPCALGTLGASHNLCPVGCCPARAPRPAAAGADSPYA*
```

Figure 1-12. Crystal structure of human ferrochelatase homodimer. Amino terminus is shown in orange, carboxy terminus is shown in cyan, and core region is shown in red and blue for chains A and B, respectively. The iron sulfur clusters are shown as green balls. Also shown is the coordination of the iron sulfur cluster by cysteines 196, 403, 406, and 411 (black sticks). Figure constructed using Pymol and PDB code 1HRK.

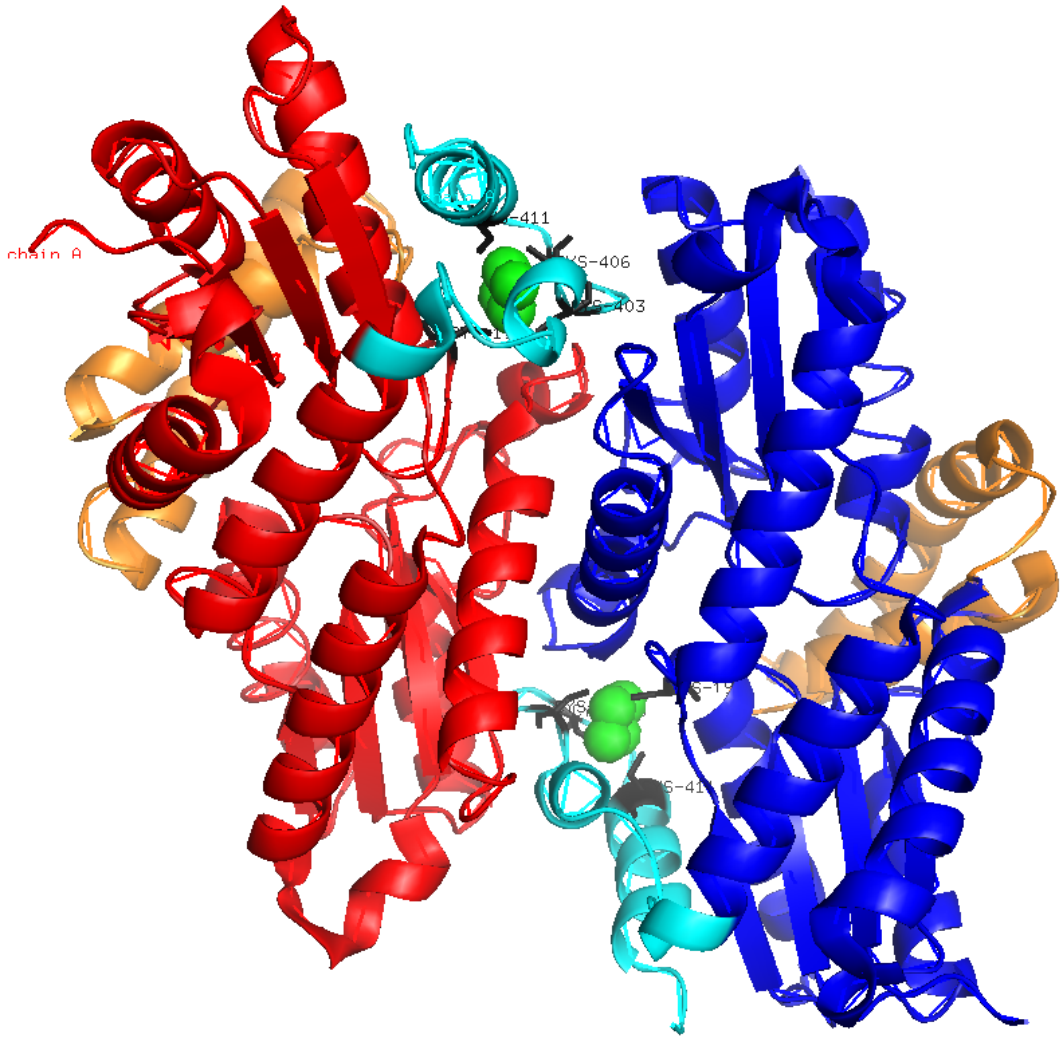
chain A
-411
S-406
-403

Figure 1-13. Ferrochelatase monomer showing the active site composition. Upper lip residues 90-130 shown in magenta, lower lip residues 300-311 shown in yellow. Also shown is the active site H263 shown as a red stick. Conserved residues R164, Y165, H341, E343, H341are shown in salmon. The [2Fe-2S] cluster is shown as green spheres. Also shown is the approximate location of the mitochondrial inner membrane. The product heme is modeled into the active site. Figure constructed using PyMol (DeLano, 2004) and PDB code 1HRK.

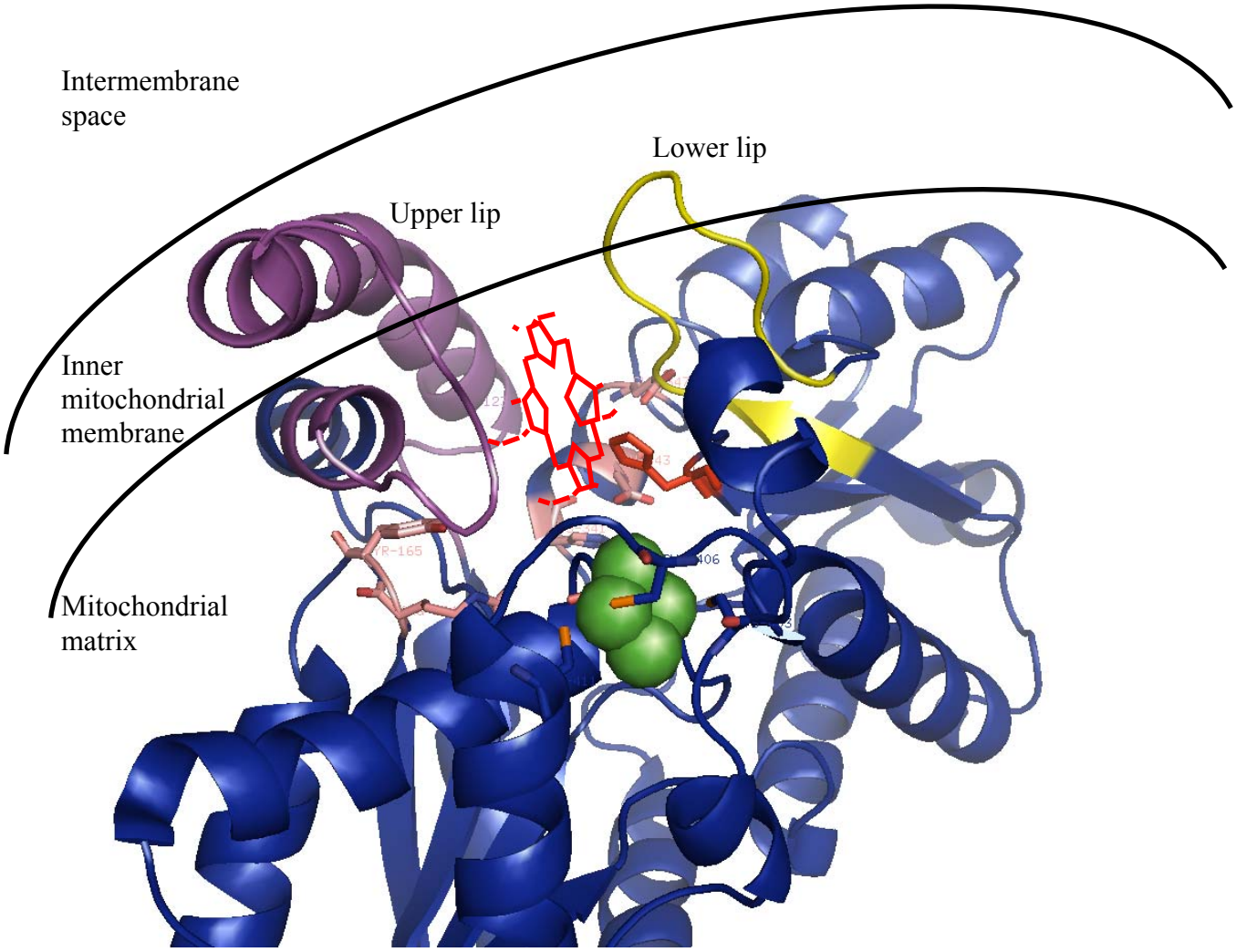
Intermembrane space
Lower lip
Upper lip
Inner mitochondrial membrane
Mitochondrial matrix

Table 1-2. Conserved residues of ferrochelatase (human numbering). This analysis is based upon 44 eukaryotic and prokaryotic ferrochelatase sequences in public databases. Identical residues represent >95% occurrence among the compared sequences. Highly conserved residues represent >95% conservative replacements among the compared sequences. Adapted from Dailey and Dailey (2003).

Identical residues	Highly conserved residues	
G77	V85	L265
P79	F88	G273
D95	L89	D274
R115	L107	V287
Y123[a]	I111	W301
S130	I132	G306
P131	G127	L311
H263[a]	G128	D316
P266	R164 [a]	P334
Y276	Y165[a]	D340
Q302	P168	I342
S303	M177	T344
W310	P192	L345
L311	S195	E347
P313	W227	I348
F337	I241	L381
E343 [a]	S261	V385

[a]Conserved hydrophilic residues located at the bottom of the active site pocket.

Figure 1-14. Overlay of the crystal structure of unbound and porphyrin-bound (E343K) ferrochelatase. This figure shows the positional changes of numerous active site residues upon binding of porphyrin. Green cartoon is E343K (bound with protoporphyrin), cyan cartoon is unbound normal enzyme; Salmon, M76; Red, H263C; Cyan and green, Y123; Yellow, S130; Magenta, R164; Teal, Y165; Blue, F337; Orange, H341; Pink and ruby helices, residues 349-361 (E343K and WT, respectively); White, protoporphyrin IX. Figure constructed using PyMol and PDB codes 2HRE and 2HRC.

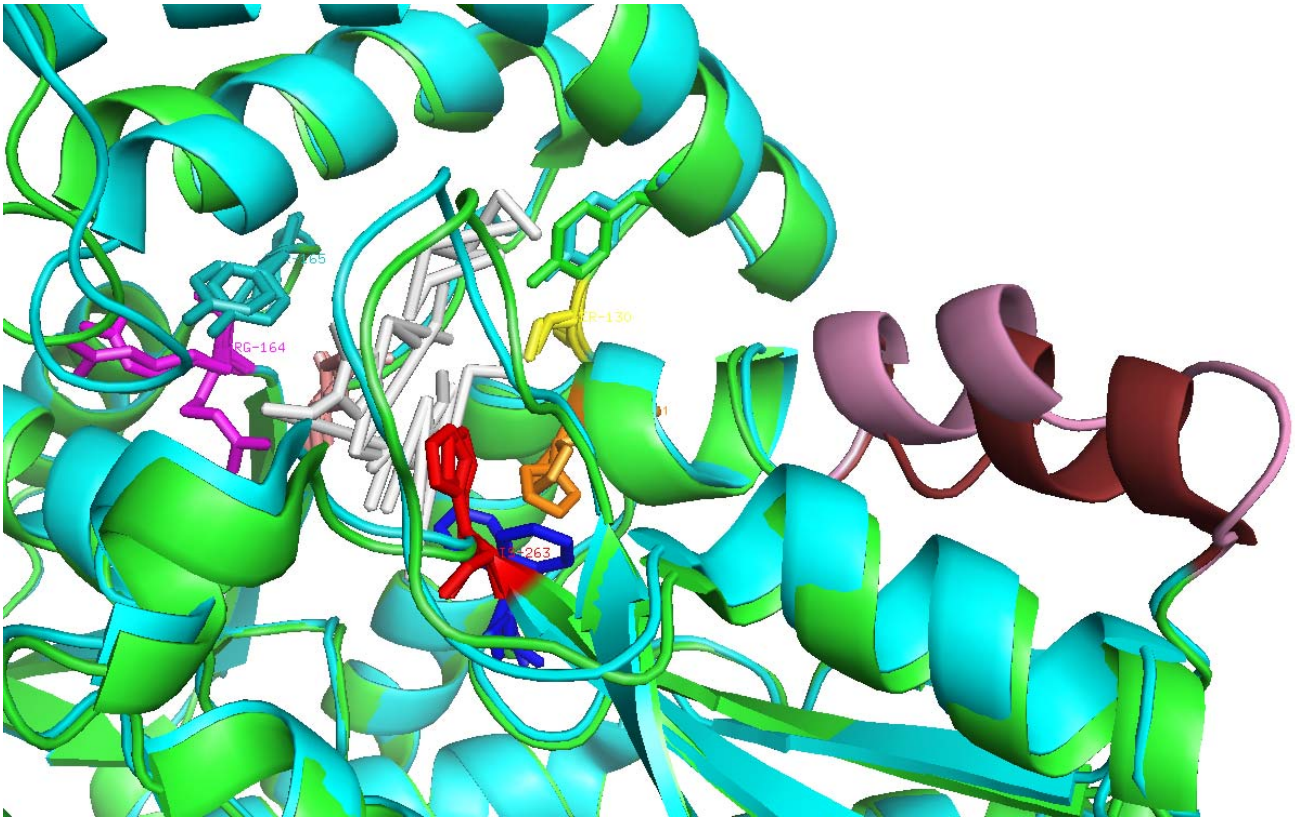
RG-164
TS-263

CHAPTER 2

IN VIVO ANALYSIS OF WILD-TYPE AND VARIANT HUMAN FERROCHELATASES [1]

[1]Ross, T.A. and Dailey, H.A. To be submitted to *J. Biol. Chem.*

ABSTRACT

Ferrochelatase is the terminal enzyme in the heme biosynthetic pathway and catalyzes the insertion of ferrous iron into protoporphyrin IX in the formation of protoheme IX. Little is known about how substrate iron is acquired and taken up by the enzyme or how the enzyme functions at the cellular level. Here we investigated the putative roles of several amino acid residues *in vivo* by constructing and analyzing site-directed mutants within the C-terminus, on the protein surface, and inside the active site of human ferrochelatase. *In vivo* function of the enzyme was assessed by monitoring complementation, cellular growth rates, and heme production in a ferrochelatase-deficient strain of *Saccharomyces cerevisiae*. The data suggest a possible surface site that may be involved in ferrochelatase function. These initial *in vivo* characterizations may lead to future advances in identifying specific amino acid residues that play a role in ferrochelatase function.

INTRODUCTION

Heme production is indispensable for life as it is a major component of a number of hemoproteins that are required for biological processes. These processes range from oxygen binding and transport, respiration and detoxification of reactive oxygen species, electron transfer, and nitrogen fixation (Grimm, 2003; Voet and Voet, 2004). Nearly all living organsms require the production of heme, the exception being a few pathogenic bacteria, extreme thermophiles, some anaerobic prokaryotes, and certain auxotrophic unicellular organisms.

Ferrochelatase (E.C. 4.99.1.1) is the final enzyme in the heme biosynthetic pathway. It is responsible for catalyzing the insertion of ferrous iron into protoporphyrin IX to form protoheme IX. In animals the protein is nuclear-encoded and via an amino-terminal mitochondrial targeting sequence is translocated to the mitochondrial matrix (Dailey, 1990; Dailey et al., 2000; Karr and Dailey, 1988). Within the mitochondria, the targeting sequence is removed, and the mature protein associates with the matrix side of the inner mitochondrial membrane through a segment of hydrophic residues within a "lip" region (Dailey, 1990; Dailey et al., 2000; Karr and Dailey, 1988). Animal ferrochelatases function as homodimers with a molecular weight of 86 kD (Wu et al., 2001). The protein contains one [2Fe-2S] cluster per monomer, and this is coordinated by three cysteine residues that are located at the carboxyl termini, and a fourth cysteine that is internal (Crouse et al., 1996; Sellers et al., 1998). Both clusters are located near the dimer interface. The active site of each monomer is a pocket with its opening facing the mitochondrial membrane. It has been proposed that ferrochelatase may acquire its porphyrin substrate directly from the previous pathway enzyme, protoporphyrinogen oxidase, which is located on the opposite side of the inner mitochondrial membrane (Dailey, 1990; Dailey and Dailey, 2003; Ferreira et al., 1988; Proulx et al., 1993). The ferrous iron substrate has been postulated to be delivered by a putative docking protein through the matrix-facing surface of the enzyme (Dailey and Dailey, 2003; Shaw et al., 2006; Yoon and Cowan, 2004). The putative docking protein previously suggested to play this role is mitoferrin, an integral membrane protein and a member of the vertebrate mitochondrial solute carrier family (Muhlenhoff et al., 2003; Shaw et al., 2006; Zhang et

al., 2005) (Figure 1). This would be consistent with two independent substrate acquisition sites.

The exact mechanism of how the iron is acquired by ferrochelatase for incorporation into the tetrapyrrole center remains to be determined. Since iron does not diffuse through the phospholipid membrane and because it is not free in the cell, due to its potential toxicity, it is possible that mitoferrin interacts directly with ferrochelatase to deliver the ferrous ion. Since the determination of the crystal structure of human ferrochelatase in 2001 (Wu et al., 2001), mutagenesis and kinetic studies have implicated sites on the surface that may be responsible for acquiring the iron ion from the putative donor protein (Najahi-Missaoui, 2003; Sellers et al., 2001). It is proposed that once the metal is bound at the protein surface, the iron is translocated through a tunnel that leads to the active site (Missaoui and Dailey, unpublished data). Studies which investigate possible regions of ferrochelatase where mitoferrin might dock would help to support a model for iron acquisition.

In vitro and *in vivo* studies have previously been carried out on the soluble bacterial ferrochelatase from *Bacillus subtilis* (Olsson et al., 2002). Data obtained in this study suggest that a surface residue plays a role in either substrate acquisition or product delivery to other proteins. Additionally, similar analysis was done with the budding yeast *Saccharomyces cerevisiae* (Gora et al., 1996). The latter data identified a region that may contribute to the metal or protoporphyrin binding domain. Additionally, Gora et al. (1996) showed that while there was correlation between activities of some variants measured *in vitro* versus *in vivo*, there was one mutant that was normal *in vitro*, but *in vivo* the mutant had a decrease in activity. This discrepancy is important since it

indicates that there may be differences between what is observed *in vitro* and what really occurs *in vivo*. A possible explanation for such a discrepancy is that a multi-protein system is required for iron delivery to ferrochelatase *in vivo* that is not required in *in vitro* enzyme assays where purified protein is supplied with excess ferrous iron substrate in solution. This iron may enter the active site, which is now solvent exposed, without the need for the donor protein. Previous *in vitro* studies on purified recombinant human ferrochelatase variants identified a set of residues that were proposed to be involved in substrate-iron binding (Sellers et al., 2001). The kinetic data for alanine replacements at residues H231 and D383 showed that both had a decreased affinity for iron (Sellers et al., 2001). However, since this site is distant from the active site, it was postulated that a path of conserved residues leading from H231/D383 to the active site may participate in movement of the iron molecule to the protein interior. These variant enzymes were not examined *in vivo* for their ability to function in a native environment.

In the current work, we examined the hypothesis that surface residues play a role *in vivo* via protein-protein interactions with an iron-donating protein. Specific variant forms of the protein were examined based on previous kinetic analysis (Sellers et al., 2001) as well as sequence and structural examination. The *Δhem15* ferrochelatase-deficient yeast strain was employed to determine if any of these mutations had an impact on the ability of the variant ferrochelatase to function *in vivo*. Since the *Δhem15* strain lacks the ability to synthesize heme and, therefore, lacks functional mitochondria, it is only able to grow fermentatively in the absence of exogenous heme. However, when complemented with functional ferrochelatase it is able to respire. The data acquired

suggest that a set of surface-located residues which have no appreciable effect on *in vitro* measured activity may be important for proper *in vivo* functioning.

MATERIALS AND METHODS

Yeast/human ferrochelatase plasmid construction. The high- and low-copy yeast shuttle vectors pRS425 and pRS316, respectively (gifts from C. Glover and W.K. Schmidt, University of Georgia), were utilized in the construction of mutant human ferrochelatase proteins as follows. pRS425 was modified by introducing a PCR generated NcoI restriction site and subsequently digested with NcoI and NotI restriction endonucleases. The previously cloned recombinant full-length *S. cerevisiae* ferrochelatase gene, and yeast upstream promoter plus mitochondrial targeting sequence (Prasad and Dailey, 1995) were PCR amplified and visualized by gel electrophoresis. The approximately 350 bp product consisting of the yeast ferrochelatase promoter and targeting sequence was extracted from the gel, purified using a QIAquick gel extraction kit (Qiagen, Valencia, CA), digested with NotI and NcoI restriction endonucleases, and ligated into pRS425. The human ferrochelatase gene was subcloned into pRS425 using the restriction sites NcoI and HindIII. Subsequently, the ferrochelatase gene along with the upstream yeast promoter and leader sequence was sub-cloned into pRS316 using restriction sites NotI and HindIII. Mutants were constructed by using the wild-type human ferrochelatase/pRS316 vector as template and QuikChange mutagenesis (Stratagene, Valencia, CA). All mutations were verified by sequence analysis (Integrated Biotech Laboratories, University of Georgia). *E. coli* strain JM109 (Promega, Madison, WI) was used as the host for plasmid cloning.

Yeast Strains and Growth Conditions. The wild-type *S. cerevisiae* strain DY1457 (*MATa, ade6, can1, his3, leu2, trp1, ura3*), ferrochelatase-deficient strain (*Δhem15*) (gifts from J. Kaplan and R.J. Crisp, University of Utah), and *Δhem15* strain containing plasmid-encoded ferrochelatase genes were used in this study (Table 1). Cells were grown at 30ºC with vigorous shaking in complete medium (1% yeast extract, 1% bactopeptone) with 3% glycerol (YPGly) as a carbon source (the final pH was approx. 6.5). In the *Δhem15* strain lacking ferrochelatase-encoded plasmid, media was supplemented with 1.5 mg/ml hemin (Sigma, Saint Louis, MO) made fresh in 0.1 N NaOH and filter-sterilized.

Complementation and Growth Analysis. Competent *Δhem15* cells were made and transformed with wild-type and mutant ferrochelatase plasmids using the Frozen-EZ Yeast Transformation II kit (Zymo Research, Orange, CA). Cells were plated and selected on CM-Uracil. Plates that did not produce colonies had plasmids that were unable to complement the *Δhem15* mutation. Cells that contained complementing plasmids were cultivated in YPGly and grown overnight to mid-log phase (approx. 0.6-1.0 OD at 600 nm). Mid-log cells were diluted to 0.05 OD with fresh YPGly media and grown at 30ºC with shaking. Cell growth was monitored for 24 hours, and the cell doubling times were determined.

Heme Content. Whole cell cytochrome content was estimated by using a modified version of the previously described pyridine hemochromagen method (Berry and Trumpower, 1987). Yeast cells harboring the ferrochelatase variants were grown and harvested in mid-log phase. Cells were spheroplasted using zymolyase with the protocol provided by MP Biomedicals (Solon, OH). Total protein content of spheroplasts was

measured using the BCA assay procedure (Pierce, Rockford, IL). Duplicate samples were used in the hemochromagen assays: 1 ml of a 200 mM NaOH stock solution and 400 µl of 40% (by volume) pyridine were added to a 1 ml aliquot of spheroplasts and mixed to solubilize the membranes and extract the hemes. The sample mixture was separated into two samples in 1-ml cuvettes. To one cuvette, 2-5 mg solid Na-dithionite (reduced sample) was added. Nothing was added to the second cuvette (oxidized sample). Using a CaryWin UV spectrophotometer, the difference spectra of Na-dithionite-reduced minus oxidized cells was recorded at room temperature from 400-650 nm. This method allows for the quantitation of cytochrome content (and therefore heme contents). The ~550 nm peak and the total cellular protein concentration were used to calculate the total amount of cytochromes *b* + *c* since they represent the major heme pools.

RESULTS

Establishment of *in vivo* test system

The primary goal of this study was to develop, test, and utilize a system whereby the functionality of human ferrochelatase variants could be examined *in vivo*. The choice of human ferrochelatase, rather than yeast ferrochelatase, was driven by the fact that significantly more data and variant ferrochelatases are available for the human protein than the yeast protein. Given that yeast ferrochelatase does not possess a [2Fe-2S] cluster as does the human enzyme and that the human enzyme is not active unless there is a cluster, it was first necessary to determine if the human wild-type ferrochelatase could complement the yeast ferrochelatase-deficient strain.

A low copy number expression vector was employed to ensure that near normal amounts of the exogeneously supplied ferrochelatase would be produced. Full length wild-type yeast (as a positive control) and human ferrochelatase with the yeast ferrochelatase mitochondrial targeting sequence were cloned into the low-copy vector, pRS316. The plasmids were transformed into the *Δhem15* strain and the cells selected on CM-Ura to ensure that the human ferrochelatase gene could effectively rescue the null strain. Colonies were observed after approximately 48 hours for cells containing both yeast and human ferrochelatase encoding plasmids. Cells that did not contain plasmid-encoded ferrochelatase and cells that contained only empty vector did not support growth of *Δhem15*. While the results showed that human ferrochelatase is capable of complementing *Δhem15*, the mere presence of colonies after 48 hrs did not demonstrate if human ferrochelatase functions as well as the yeast enzyme. Therefore, these strains were grown non-fermentatively, and the rates of cell growth were monitored over 24 hours. Results showed that the cell doubling times of yeast containing human ferrochelatase were similar to those with yeast ferrochelatase (Table 2).

In vivo examination of ferrochelatase variants

Active site and cluster-associated variants

With the knowledge that wild-type human ferrochelatase is fully functional in yeast it became possible to examine *in vivo* the possible roles of selected human ferrochelatase residues. The variants first examined fall into three major categories: those present in the active site, those near the carboxyl-terminal end of the protein, and those on the protein surface. Of the active site residues, H263 has been proposed to be

essential for catalysis based on kinetic analysis (Sellers et al., 2001). Any residue replacement of H263 results in total loss of enzyme activity. Additionally, it has also been shown that mutants homologous to the human H263 residue in *Drosophila melanogaster* and *E. coli* have no measurable activity (Gora et al., 1996; Sellers et al., 2001). Thus the human ferrochelatase H263C variant was employed as an internal negative control.

R164 and Y165, which are located across the active site pocket from H263, have been implicated in metal coordination and delivery to the porphyrin center (Sellers et al., 2001). The double mutant variant R164L/Y165F was investigated *in vivo.* The R→L substitution at 164 removes the positive charge and introduces a non-polar side chain while the Y→F substitution at 165 maintains the structure but removes the polar hydroxyl group. Our results showed that the R164L/Y165F double mutant was unable to rescue *Δhem15*. Cells transformed with the R164L single substitution variant had a cell doubling time similar to wild-type ferrochelatase and produced normal amounts of heme whereas Y165F single substitution variant yielded a 64% increase in cell doubling time and 44% less heme compared with wild-type enzyme (Figure 2).

Carboxyl-terminal residues previously shown to be involved in coordination of the iron-sulfur cluster and/or homodimer stability (Dailey et al., 1994; Sellers et al., 1998) were investigated. Ferrochelatase variant C406S, one of the four cluster-ligating residues, and F417S, implicated in the human genetic disease erythropoietic protoporphyria (EPP) (Brenner et al., 1992) were examined. Previous work has demonstrated that the F417S mutation lacks the [2Fe-2S] cluster and has minimal activity *in vitro*(Dailey et al., 1994; Najahi-Missaoui, 2003; Sellers et al., 1998). To examine the

physiologic function of the two variants, F417S and C406S, *in vivo* analysis was carried out, and it was found that neither variant was functional, as they did not complement the ferrochelatase-deficient yeast strain. This is consistent with data from *in vitro* analysis (Dailey et al., 1994; Sellers et al., 1998).

Surface variants

Since our hypothesis is that *in vivo* there exist protein-protein interactions between ferrochelatase and some iron donor molecule, a selection of surface residues was examined. Variants of the residues selected should show little or no effect on *in vitro* measured activity so that any *in vivo* effects would be attributed to something other than actual enzyme catalysis. We examined two potential sites on the protein surface that may be involved in ferrochelatase function. The selection of these sites was based on two observations: 1) human ferrochelatase functions normally in yeast, and 2) yeast ferrochelatase functions normally in zebrafish (personal communication, Barry Paw). These observations imply that if there are protein-protein interactions between ferrochelatase and another protein, then the points of contact must be conserved among these three ferrochelatases or else they would not be functionally interchangeable. In this regard it should be noted that ferrochelatases are not universally interchangeable. The enzyme from *Bacillus subtilis* does not complement yeast cells defective in ferrochelatase activity (Gora et al., 1999). Examination of the crystal structure of ferrochelatase from human and yeast along with the primary sequences of human, yeast, and zebrafish (Figure 3) yields a limited number of identical surface residues, which are clustered in two main regions near D383 and H240 (Figure 4). These two residues have previously

been suggested to be involved in iron acquisition through cobalt-soaking experiments (Wu et al., 2001) and kinetic analysis (Najahi-Missaoui, 2003; Sellers et al., 2001).

Residues within each of these regions were selected for mutagenesis. Variants were designed to alter residue side chain size and charge, or to change the polar characteristic of the side chain. Both single and double surface mutation variants were examined. Each variant is listed in Table 3.

Characteristics of R366, E369, H240. The residue H240 is located on the back side of the enzyme from the mouth of the active site, and at the end of a tunnel that extends from the active site to the protein surface (Figure 5). The adjacent E369 is identical between human, yeast, and zebrafish ferrochelatase, and the conserved R366 is located within 13 angstroms of H240. We analyzed variant forms of ferrochelatase with engineered mutations at these three residues (H240A, H240E, E369T, H240A/R366E, H240A/E369K, H240A/E369T). As shown in Figure 6A, near-normal activity was seen with H240A as it had a doubling time and relative heme synthesis level of 3.7 hours and 89%, respectively. When the H240 residue was replaced with glutamate, changing its imidazolium moiety to a negatively charged functional group, a 44% decrease in heme synthesis was observed. E369T had a slightly higher doubling time than the normal enzyme while the amount of heme production was decreased by 14%. The most significant cellular defects were displayed when the simultaneous mutations H240A/R366E, H240A/E369K and H240A/E369T were introduced. For the H240A/R366E variant, the doubling time was not drastically altered; however, the amount of heme synthesized was only 53% of that produced by the wild-type enzyme. The doubling time was higher and heme production was lower than normal for both the

H240A/E369K and H240A/E369T variants, with H40A/E369T having a more pronounced heme dysfunction (Figure 6A).

Characteristics of H231, D383. H231 is located opposite D383 and was mutated to alanine. As shown in Figure 6B, H231A had both growth and heme synthesis defects. D383A was mostly affected in heme production while D383K had normal heme production, but showed an increase in cell doubling time. When the two residues were mutated simultaneously to H231A/D383A and H231A/D383K there was no dramatic change in the amount of heme synthesized by these cells. Notably, H231A/D383K had a higher cell doubling time than wild-type enzyme.

Characteristics of E289, R290. Model docking studies done by others identified the region containing E289 and R290 as a potential site involved in protein docking with a putative iron-donating protein. When the mutations E289K, R290E, and E289A/R290A were investigated, data showed that the amount of heme synthesized by these cells was normal, although the cells had higher cell doubling times (Figure 7).

DISCUSSION

The catalytic cycle for the enzyme ferrochelatase is relatively well understood. Catalysis is thought to occur through a sequential bi-bi reaction (Dailey and Fleming, 1983; Hoggins et al., 2007). Metallation is proposed to involve desolvation of substrate iron, porphyrin macrocycle distortion, and metal insertion. For substrate iron to be incorporated, it must undergo several metabolic events: (1) import into the mitochondria, (2) delivery to ferrochelatase, (3) translocation into the active site, and (4) insertion into the tetrapyrrole center. The exact mechanism by which ferrochelatase acquires and

utilizes substrates remains to be elucidated. Kinetic and modeling studies based upon the crystal structures of human ferrochelatase and tobacco protoporphyrinogen oxidase suggest that acquisition of the porphyrin substrate occurs via direct, but transient, contact between these two enzymes across the inner mitochondrial membrane (Ferreira et al., 1988; Koch et al., 2004). Also, there is now good evidence about how product is released following catalysis (Dailey et al., 2007; Medlock et al., 2007; Wu et al., 2001). However, little is known about iron acquisition and transport to the active site prior to metalation. A possible site for initial iron binding at the surface of human ferrochelatase has previously been proposed based on mutagenesis, kinetic studies, and structural information (Najahi-Missaoui, 2003; Sellers et al., 2001; Wu et al., 2001), but has never been tested *in vivo.* In the current study a ferrochelatase-deficient strain of *S. cerevisiae* was employed to examine the activity of human ferrochelatase variants *in vivo.* Our goal was to identify residues that may be important for protein-protein interactions, presumably in the supply of substrate iron to ferrochelatase.

Prior to the actual testing of variants, it was necessary to determine if human ferrochelatase can function to replace yeast ferrochelatase *in vivo.* One difference between ferrochelatase of the budding yeast *S. cerevisiae* and human ferrochelatase is that the human enzyme possesses a [2Fe-2S] cluster whereas *S. cerevisiae* does not possess a cluster. While the human enzyme is catalytically active only when there is an intact cluster, the function of the cluster is currently not known, although it has been implicated as a sensor for nitric oxide (Sellers et al., 1996). When the wild-type plasmid-encoded recombinant human ferrochelatase gene is expressed in ferrochelatase-deficient yeast cells, the exogenously supplied protein was able to complement the mutant strain.

This demonstrates that the yeast cells are able to synthesize and incorporate the cluster into the human ferrochelatase protein even though the yeast host does not synthesize [2Fe-2S] clusters for its own ferrochelatase. Additionally, it has recently been demonstrated that yeast ferrochelatase can functionally complement ferrochelatase-deficient zebrafish (personal communication, Barry Paw). These observations are of significance since they strongly imply that any residues involved in protein-protein interactions are conserved across these three organisms and that there must be a site on the surface that is common to all the enzymes which allows for a putative docking protein to bind or associate with the surface for delivery of the iron.

Previously the surface residues H231 and D383 have been suggested to be involved in iron binding since a cobalt ion is found associated with this region in the crystal structure (Wu et al., 2001) and the kinetic parameters for iron are altered in enzyme variants with mutations at these residues (Sellers et al., 2001). However, the *in vivo* activities of H231A/D383A and H231A/D383K show that protein function is not severely affected by these changes (Figure 6B and Table 4). This may be consistent with the *in vitro* kinetic determinations that found an increased K_m for iron, but also an increase in k_{cat}. Interestingly, while D383 is conserved across species, H231 is not conserved between human, yeast, or zebrafish (Figure 3). E289, another surface residue examined in the current work, is also not conserved with yeast and zebrafish, which contain glutamine and aspartic acid, respectively, at this location. Additionally, it may be difficult for a molecular interaction to occur at the E289/R290 site due to steric constraints at this site near the dimer interface (Figure 4).

There is one group of surface-located residues that are conserved, and when these are mutated the resultant variants expressed in ferrochelatase-deficient yeast yield altered growth and/or heme production (Figure 6A and Table 4). These residues, H240, E369 and R366, occupy a site on the back surface of the enzyme at the entrance of a tunnel that extends to the back of the active site pocket. We propose that this charged patch is a recognition site for a putative iron donating protein, possibly mitoferrin. Alteration in residues at this site have an impact on the interaction between ferrochelatase and the iron donor that is trivial in an *in vitro* enzyme assay where excess ferrous iron is available in the absence of the donor protein. The fact that a second patch of relatively conserved charged residues exist at a site near to, but distinct from the H240/E369/R366 patch, suggests that the overall recognition site for protein-protein interactions may be larger than just one small region. Such a hypothesis is certainly consistent with other well characterized protein pairs (Janin and Chothia, 1990; LoConte et al., 1999; Sheinerman et al., 2000). In order to ascertain if these sites are indeed involved with protein-protein interactions, it will be necessary to identify the iron donation protein and characterize the nature of the intermolecular interaction.

In conclusion, we have developed a system for studying ferrochelatase function *in vivo* by taking advantage of a mutant form of *S. cerevisiae* that lacks ferrochelatase. The initial *in vivo* characterization of active site, carboxyl-terminal, and surface residues of human ferrochelatase represents the first attempt at identifying residues that are involved in possible protein-protein interactions.

ACKNOWLEDGMENTS

For their help with yeast methodologies, materials, and protocols as well as critical discussion we thank Drs. J. Kaplan (University of Utah), R.J. Crisp (University of Utah), P. Cobine (University of Utah), C. Glover (The University of Georgia), and W.K. Schmidt (The University of Georgia). We also wish to thank Dr. A.E. Medlock for assistance with the initial stages of this research, and T.A. Dailey and W.N. Missaoui for construction of some of the mutants.

Figure 1. Model showing the possible orientation and interaction of protoporphyrinogen oxidase (PPO), ferrochelatase (Fc), and the putative iron-donating protein mitoferrin (Mf). Substrate iron is shown as orange balls. HCP, putative heme carrier protein.

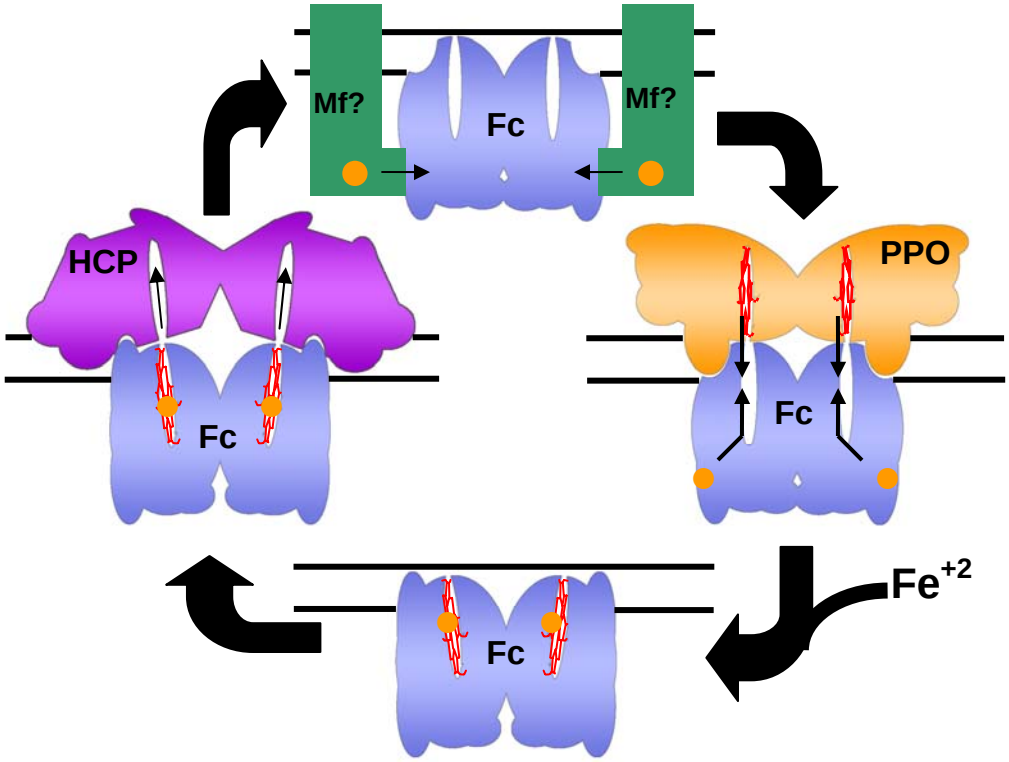

Table 1. Strains used in this study.

Strain	Genotype	Source
DY1457 (parental)	*MATa, ade6, can1, his3, leu2, trp1, ura3*	J. Kaplan
Δhem15 [a]	DY1457, *hem15::KanMX4*	J. Kaplan
Δhem15 - pHEM15	*hem15::KanMX4*, pHEM15	This study
Δhem15 - pHFC	*hem15::KanMX4*, pHFC	This study

Table 2. Validation of cell growth on the non-fermentable carbon source YPGly. DY1457, parental yeast strain; pHEM15, plasmid-encoded yeast ferrochelatase; pHFC, plasmid-encoded human ferrochelatase; *Δhem15*, ferrochelatase-deficient yeast strain; *a*, does not grow in absence of heme supplementation.

Plasmid	Carbon Source	Doubling Time (h)
DY1457 (WT yeast)	Glycerol	3.4 ± 0.5
pHEM15	Glycerol	3.4 ± 0.6
pHFC	Glycerol	3.3 ± 0.2
Δhem15 [a]	Glycerol	--

Figure 2. Cell doubling times and heme synthesis levels of wild-type and human ferrochelatase active site variants.

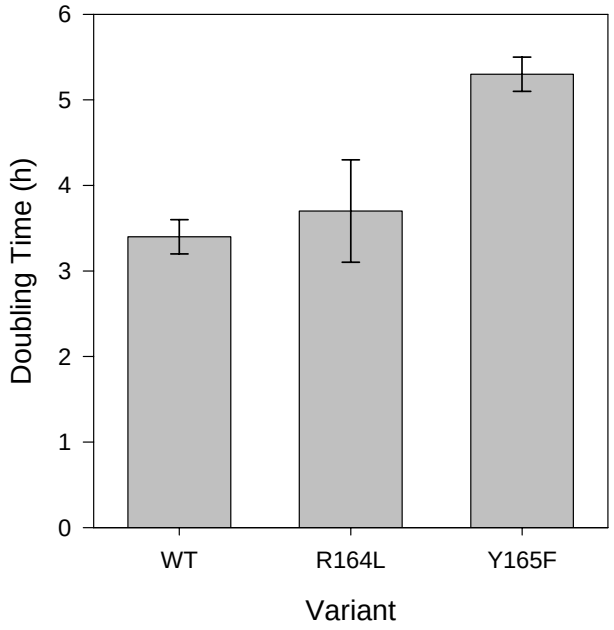

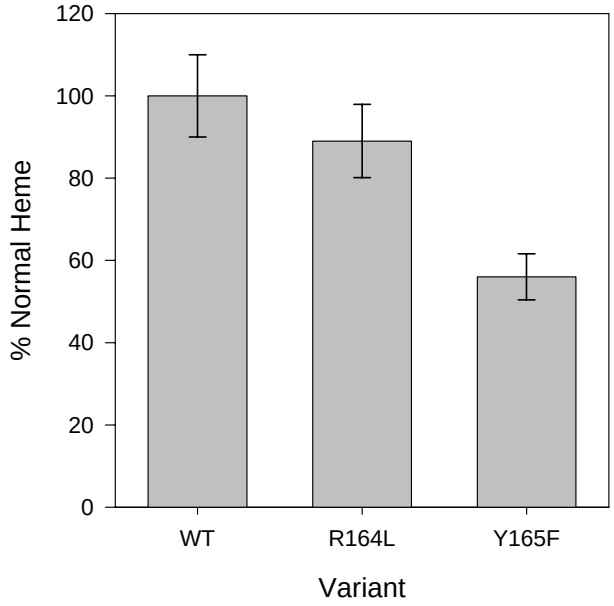

Figure 3. Sequence comparison of ferrochelatase from human, zebrafish (danio sp.), and yeast (*Saccharomyces cerevisiae)*. Astericks represent identical residues; colons represent conserved residues. Red astericks and colons represent residues examined in this study. Pileup created using CLUSTALW.

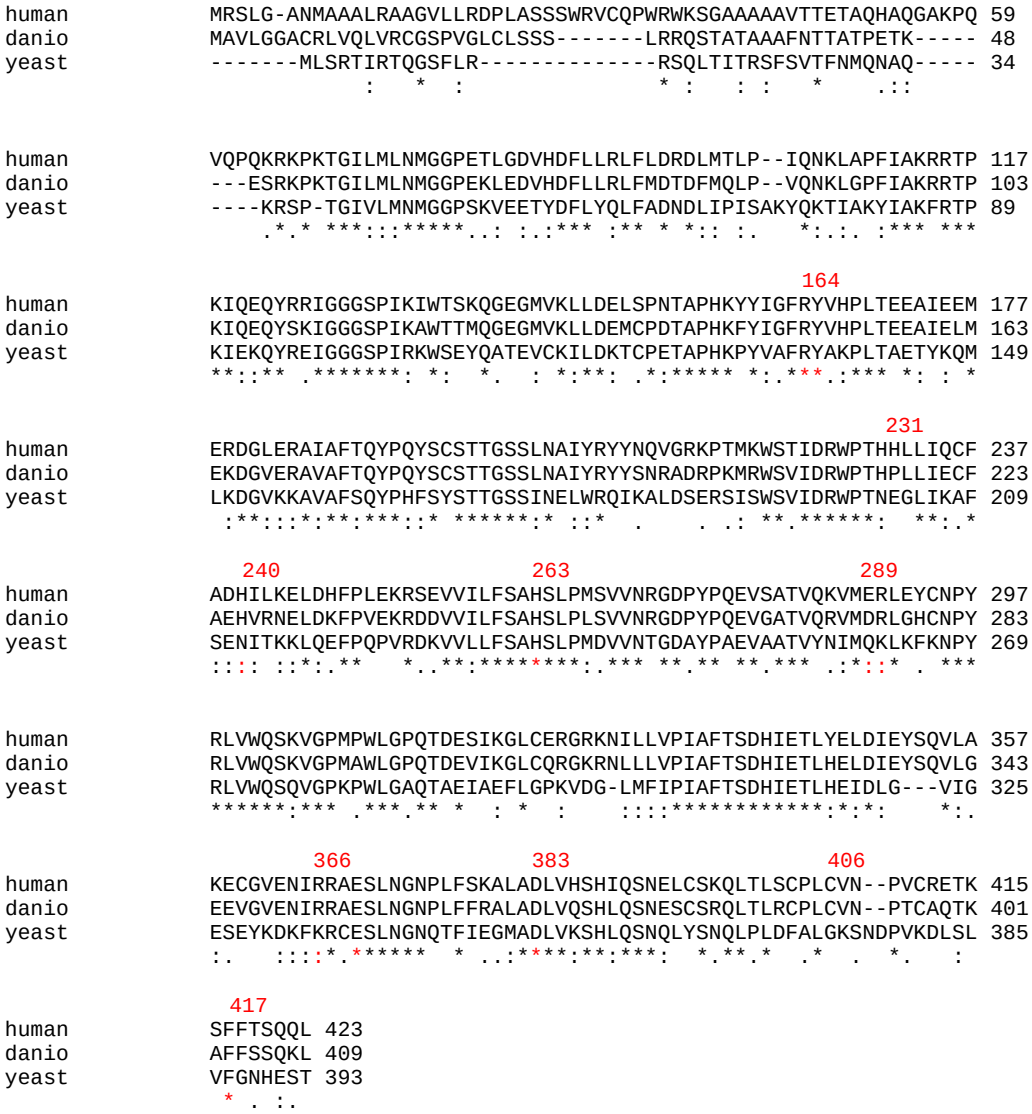

Figure 4. Crystal structure of human ferrochelatase showing the surface regions of similarity and difference between human, yeast, and zebrafish ferrochelatase. This was based on primary sequence comparisons. Red, identical residues; yellow, conserved residues; green, different residues. The porphyrin molecule is shown as burgundy dots. Figure constructed using PyMol (DeLano Scientific) and PDB codes 2HRE and 2HRC.

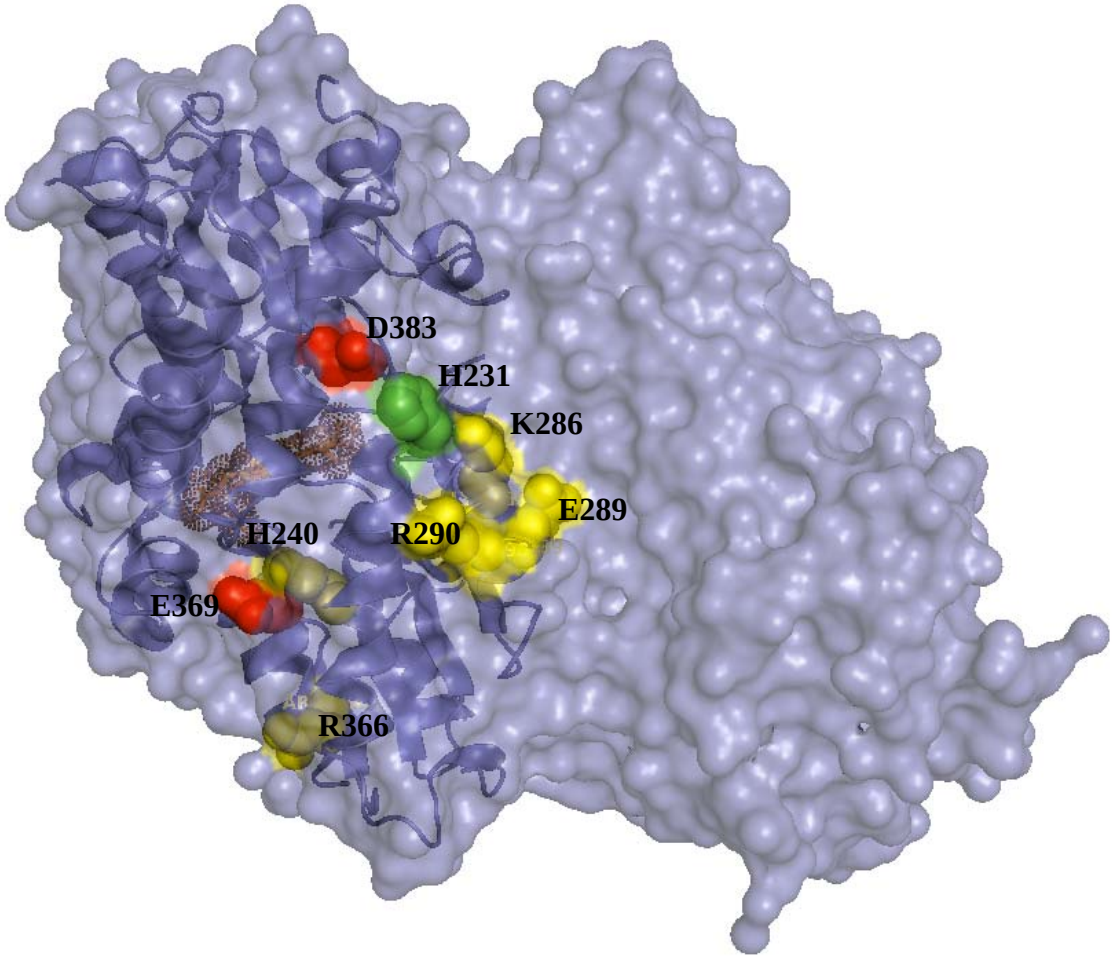

Table 2. Comparison of surface sequence similarities and differences between human, yeast, and zebrafish ferrochelatase. Astericks represent residues that were examined in this study.

Human	Yeast	Zebrafish	Comments	Human Variants examined
Identical				
E279	E251	E265		
N295	N267	N281		
D349	D320	D335	Highly conserved	
R367	R335	R353	Highly conserved	
E369*	E337	E355		E369T
D383*	D351	D369		D383A/K
Conserved				
D239	E211	E225	Acidic	
R290*	K262	R276	Basic	R290A/E
E363	E331	D349	Acidic	
R366*	K334	R353	Basic	R366E
H240*	N212	H226	Polar	H240A/E
Y346	H317	H332	Polar	
Different				
H231*	E203	P217		H231A
E289*	Q261	D275		E289A/K
K286	N258	R272		
K243	K215	N229		

Figure 5. Crystal structure of human ferrochelatase showing the tunnel that extends from the surface to the active site. H240 and E369 are shown as sticks at the bottom of the figure. A cartoon of heme is modeled into the active site and is shown as red lines. Figure constructed using PyMol (DeLano, 2004) and PDB file 2HRC.

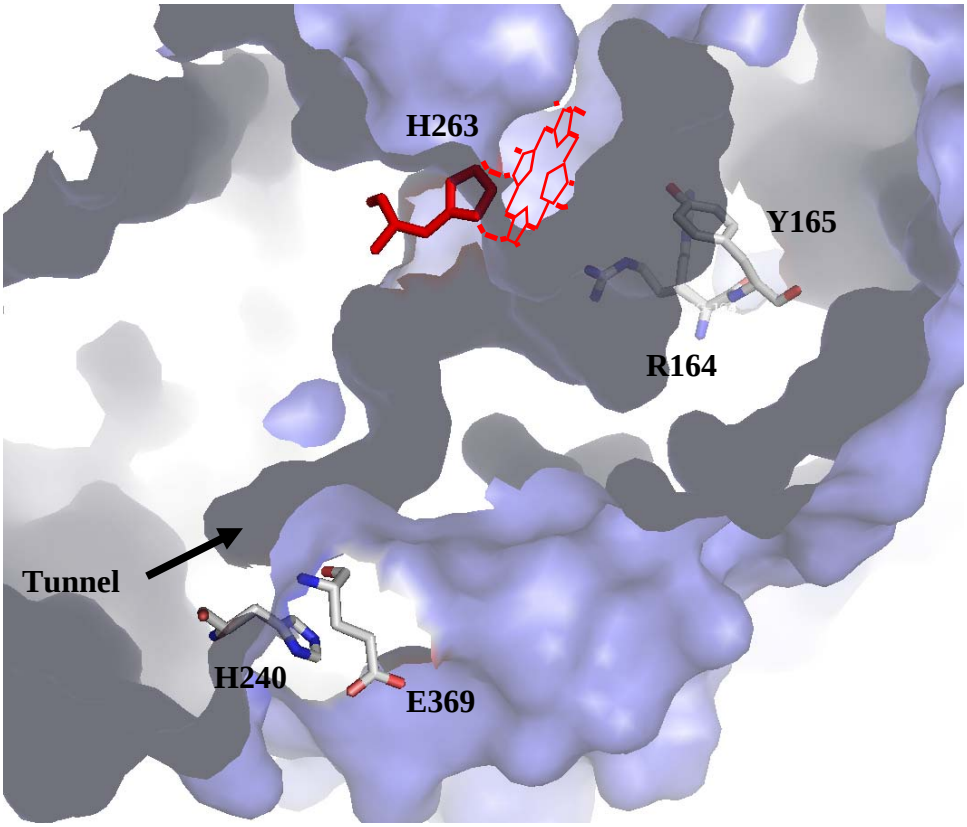

Figure 6. Cell doubling times and heme synthesis levels of wild-type and variant ferrochelatase surface residues from two independent surface sites.

A) H240 Tunnel

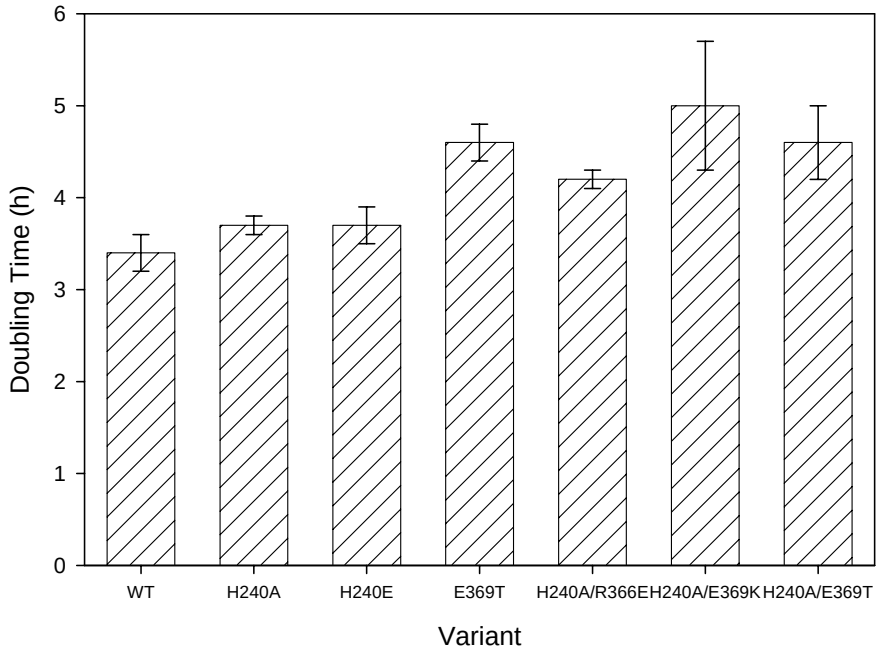

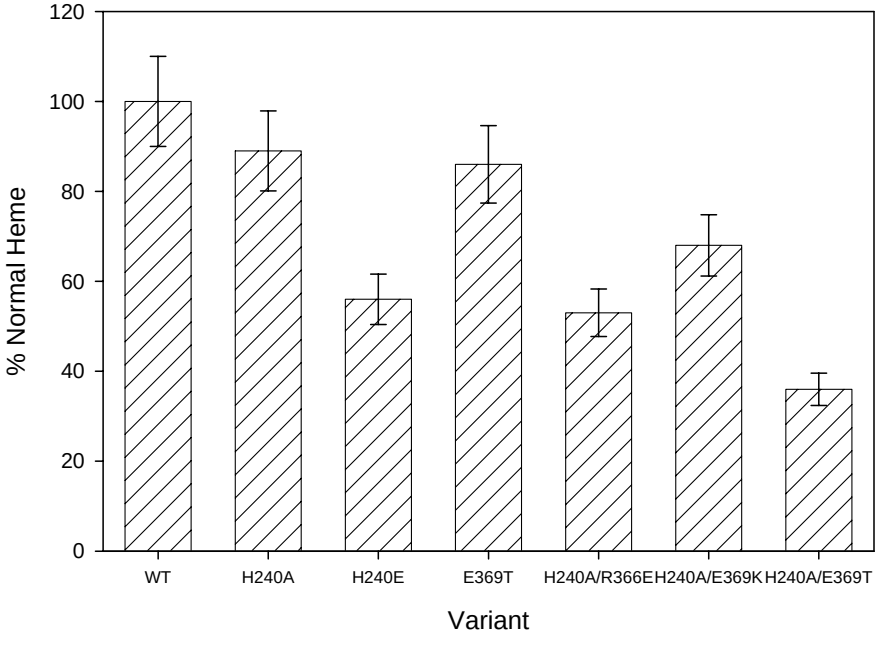

B) H231/D383 Site

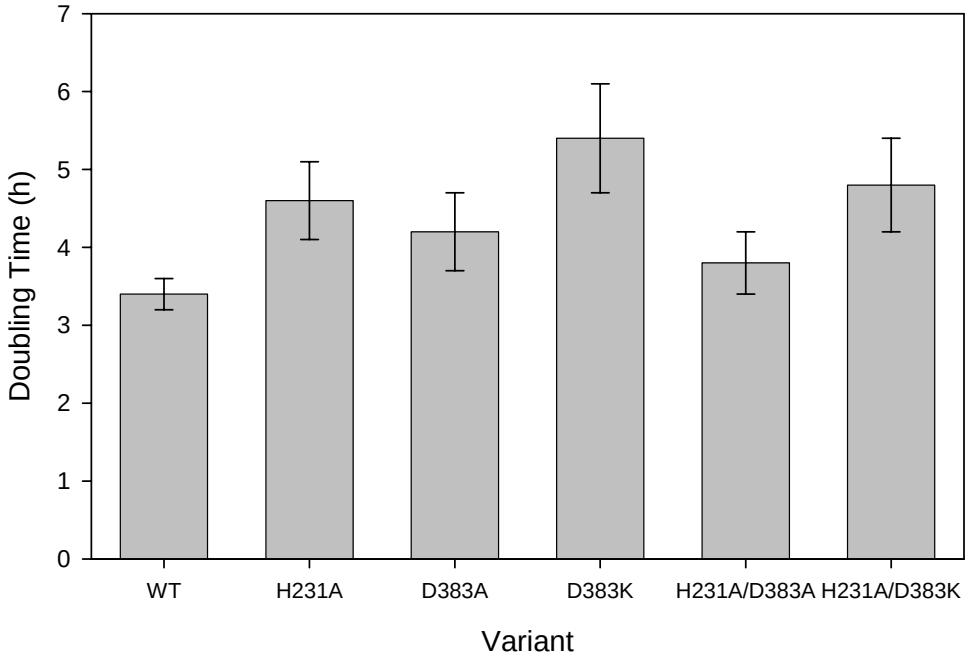

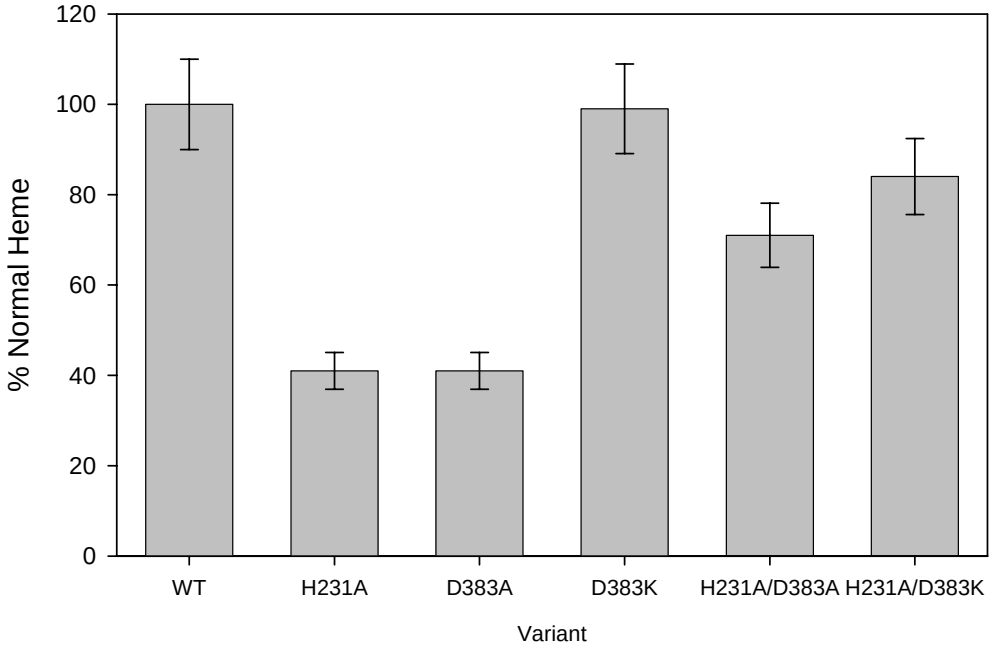

Figure 7. Cell doubling times and heme synthesis levels of wild-type and variant ferrochelatase surface residues from the dimer interface.

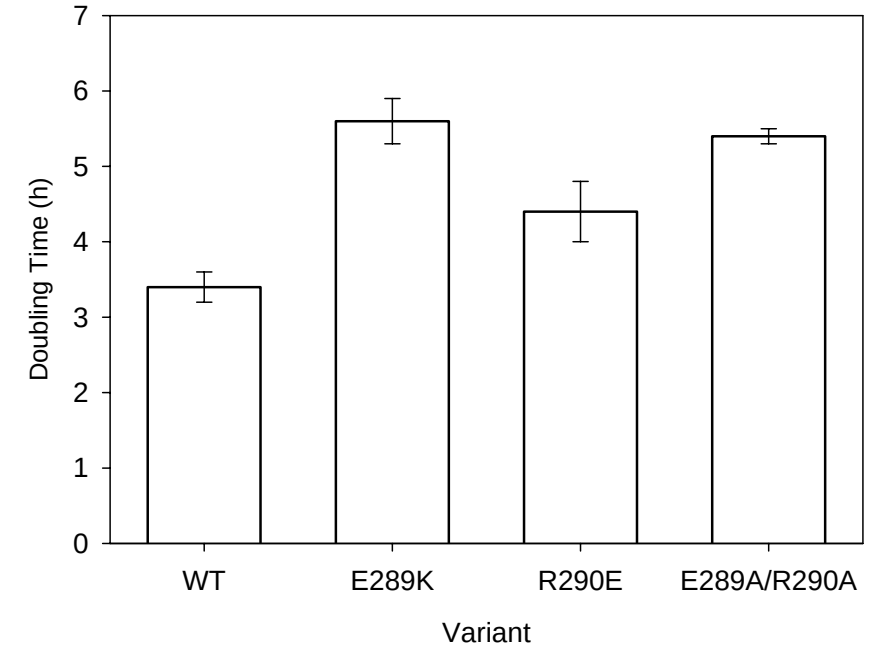

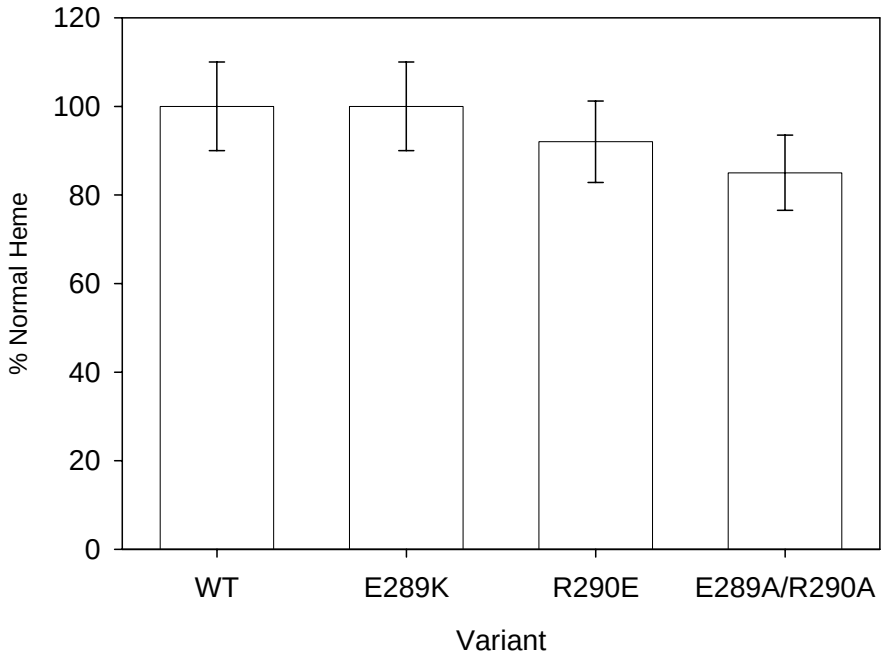

Table 3. Summary table showing results for complementation, cellular growth rates (doubling time), and heme synthesis levels of each ferrochelatase variant examined in this study. Heme synthesis values reported represent the average of three samples with <10% standard deviation.

Variant	**Complements *Δhem15*?**	**Doubling Time (h)**	**Heme synthesis (% of WT)**
Active site			
Wild-Type	yes	3.4 ± 0.2	100
R164L	yes	3.7 ± 0.6	89
R164L/Y165F	**no**	--	--
Y165F	yes	5.3 + 0.2	56
H263C	**no**	--	--
C-terminus			
C406S	**no**	--	--
F417S	**no**	--	--
Surface			
H231A	yes	4.6 ± 0.5	41
H231A/D383A	yes	3.8 ± 0.4	71
H231A/D383K	yes	4.8 ± 0.6	84
H240A	yes	3.7 ± 0.1	89
H240A/R366E	yes	4.2 ± 0.1	53
H240A/E369K	yes	5.0 ± 0.7	68
H240A/E369T	yes	4.6 ± 0.4	36
H240E	yes	3.7 ± 0.2	56
E289A/R290A	yes	5.4 + 0.1	85
E289K	yes	5.6 + 0.3	100
R290E	yes	4.4 ± 0.4	92
E369T	yes	4.6 ± 0.2	86
D383A	yes	4.2 ± 0.5	41
D383K	yes	5.4 ± 0.7	99

REFERENCES

Berry, E. A., and Trumpower, B. L. (1987). Simultaneous determination of hemes a, b, and c from pyridine hemochrome spectra. Anal Biochem *161*, 1-15.

Brenner, D. A., Didier, J. M., Frasier, F., Christensen, S. R., Evans, G. A., and Dailey, H. A. (1992). A molecular defect in human protoporphyria. Am J Hum Genet *50*, 1203-1210.

Crouse, B. R., Sellers, V. M., Finnegan, M. G., Dailey, H. A., and Johnson, M. K. (1996). Site-directed mutagenesis and spectroscopic characterization of human ferrochelatase: identification of residues coordinating the [2Fe-2S] cluster. Biochemistry *35*, 16222-16229.

Dailey, H. A. (1990). Conversion of coproporphyrinogen to protoheme in higher eukaryoes and bacteria, In Biosynthesis of heme and chlorophylls H. A. Dailey, ed. (New York: McGraw-Hill), pp. 123-163.

Dailey, H. A., and Dailey, T. A. (2003). Ferrochelatase, In The Porphyrin Handbook, K. M. Kadish, Smith, K.M., Guillard, R., ed. (California, USA: Elsevier Science), pp. 93-121.

Dailey, H. A., Dailey, T. A., Wu, C. K., Medlock, A. E., Wang, K. F., Rose, J. P., and Wang, B. C. (2000). Ferrochelatase at the millennium: structures, mechanisms and [2Fe-2S] clusters. Cell Mol Life Sci: CMLS *57*, 1909-1926.

Dailey, H. A., Finnegan, M. G., and Johnson, M. K. (1994). Human ferrochelatase is an iron-sulfur protein. Biochemistry *33*, 403-407.

Dailey, H. A., and Fleming, J. E. (1983). Bovine ferrochelatase. Kinetic analysis of inhibition by N-methylprotoporphyrin, manganese, and heme. J Biol Chem *258*, 11453-11459.

Dailey, H. A., Wu, C.-K., Horanyi, P., Medlock, A. E., Najahi-Missaoui, W., Burden, A., Dailey, T. A., and Rose, J. (2007). Altered orientation of active site residues in variants of human ferrochelatase. Evidence for a hydrogen bond network involved in catalysis. Biochemistry *46*, 7973-7979.

DeLano, W. L. (2004). The PyMol molecular graphics system, LLC (San Carlos, CA: DeLano Scientific).

Ferreira, G. C., Andrew, T. L., Karr, S. W., and Dailey, H. A. (1988). Organization of the terminal two enzymes of the heme biosynthetic pathway. Orientation of protoporphyrinogen oxidase and evidence for a membrane complex. J Biol Chem *263*, 3835-3839.

Gora, M., Grzybowska, E., Rytka, J., and Labbe-Bois, R. (1996). Probing the active-site residues in *Saccharomyces cerevisiae* ferrochelatase by directed mutagenesis. *In vivo* and *in vitro* analyses. J Biol Chem *271*, 11810-11816.

Gora, M., Rytka, J., and Labbe-Bois, R. (1999). Activity and cellular location in Saccharomyces cerevisiae of chimeric mouse/yeast and Bacillus subtilis/yeast ferrochelatases. Arch Biochem Biophys *361*, 231-240.

Grimm, B. (2003). Regulatory Mechanisms of Eukaryotic Tetrapyrrole Biosynthesis, In The Porphyrin Handbook, K. M. Kadish, Smith, K.M., and Guilard, R., ed. (San Diego: Academic Press), pp. 1-32.

Hoggins, M., Dailey, H. A., Hunter, C. N., and Reid, J. D. (2007). Direct measurement of metal ion chelation in the active site of human ferrochelatase. Biochemistry *46*, 8121-8127.

Janin, J., and Chothia, C. (1990). The structure of protein-protein recognition sites. J Biol Chem *285*, 16027-16030.

Karr, S. R., and Dailey, H. A. (1988). The synthesis of murine ferrochelatase *in vitro* and *in vivo*. Biochem J *254*, 799-803.

Koch, M., Breithaupt, C., Kiefersauer, R., Freigang, J. r., Huber, R., and Messerschmidt, A. (2004). Crystal structure of protoporphyrinogen IX oxidase: a key enzyme in haem and chlorophyll biosynthesis. EMBO J *23*, 1720-1728.

LoConte, L., Chothia, C., and Janin, J. (1999). The atomic structure of protein-protein recognition sites. J Mol Biol *285*, 2177-2198.

Medlock, A. E., Dailey, T. A., Ross, T. A., Dailey, H. A., and Lanzilotta, W. N. (2007). A pi-helix switch selective for porphyrin deprotonation and product release in human ferrochelatase. J Mol Biol *373*, 1006-1016.

Muhlenhoff, U., Stadler, J. A., Richhardt, N., Seubert, A., Eickhorst, T., Schweyen, R. J., Lill, R., and Wiesenberger, G. (2003). A specific role of the yeast mitochondrial carriers MRS3/4p in mitochondrial iron acquisition under iron-limiting conditions. J Biol Chem *278*, 40612-40620.

Najahi-Missaoui, W. (2003) Production and characterization of erythropoietic protoporphyric heterodimeric ferrochelatases, Thesis M S --University of Georgia.

Olsson, U., Billberg, A., Sjovall, S., Al-Karadaghi, S., and Hansson, M. (2002). *In vivo* and *in vitro* studies of *Bacillus subtilis* ferrochelatase mutants suggest substrate channeling in the heme biosynthesis pathway. J Bacteriol *184*, 4018-4024.

Prasad, A. R., and Dailey, H. A. (1995). Effect of cellular location on the function of ferrochelatase. J Biol Chem *270*, 18198-18200.

Proulx, K. L., Woodward, S. I., and Dailey, H. A. (1993). In situ conversion of coproporphyrinogen to heme by murine mitochondria: terminal steps of the heme biosynthetic pathway. Prot Sci *2*, 1092-1098.

Sellers, V. M., Johnson, M. K., and Dailey, H. A. (1996). Function of the [2FE-2S] cluster in mammalian ferrochelatase: a possible role as a nitric oxide sensor. Biochemistry *35*, 2699-2704.

Sellers, V. M., Wang, K. F., Johnson, M. K., and Dailey, H. A. (1998). Evidence that the fourth ligand to the [2Fe-2S] cluster in animal ferrochelatase is a cysteine. Characterization of the enzyme from *Drosophila melanogaster*. J Biol Chem *273*, 22311-22316.

Sellers, V. M., Wu, C. K., Dailey, T. A., and Dailey, H. A. (2001). Human ferrochelatase: characterization of substrate-iron binding and proton-abstracting residues. Biochemistry *40*, 9821-9827.

Shaw, G. C., Cope, J. J., Li, L., Corson, K., Hersey, C., Ackermann, G. E., Gwynn, B., Lambert, A. J., Wingert, R. A., and Traver, D. (2006). Mitoferrin is essential for erythroid iron assimilation. Nature *440*, 96-100.

Sheinerman, F. B., Norel, R., and Honig, B. (2000). Electrostatic aspects of protein-protein interactions. Curr Opin Struct Biol *10*, 153-159.

Voet, J. G., and Voet, D. (2004). Biochemistry, 3rd edn (New York: J. Wiley & Sons).

Wu, C. K., Dailey, H. A., Rose, J. P., Burden, A., Sellers, V. M., and Wang, B. C. (2001). The 2.0 A structure of human ferrochelatase, the terminal enzyme of heme biosynthesis. Nat Struct Biol *8*, 156-160.

Yoon, T., and Cowan, J. A. (2004). Frataxin-mediated iron delivery to ferrochelatase in the final step of heme biosynthesis. J Biol Chem *279*, 25943-25946.

Zhang, Y., Lyver, E. R., Knight, S. A. B., Lesuisse, E., and Dancis, A. (2005). Frataxin and mitochondrial carrier proteins, Mrs3p and Mrs4p, cooperate in providing iron for heme synthesis. J Biol Chem *280*, 19794-19807.

CHAPTER 3

SUMMARY AND CONCLUSIONS

On the basis of the data presented here, we have begun to characterize ferrochelatase surface residues that may be important in iron acquisition and/or protein recognition and have shown that the most probable site is not a single region, but instead a large, charged patch on the back of the protein. This supports the most current model of Najahi-Missaoui (2003). In order to determine if this site is part of a larger recognition site, it will be necessary to carry out further studies which may include analyzing ferrochelatase variants containing triple mutations around the H240/E369/R366 region that are identical or highly conserved among human, yeast, and zebrafish ferrochelatases. Additionally, kinetic analysis may be done to identify variants that have little effect on *in vitro* activity. Although the identification of the putative iron-donating protein remains to be determined, further *in vivo* studies may help to pinpoint more precisely the location of a protein recognition site.

REFERENCES

Najahi-Missaoui, W., and Dailey, H.A. (2005). Production and characterization of erythropoietic protoporphyric heterodimeric ferrochelatases. Blood *106*, 1098-11047.